1-1-2011

Expression of microbial rhodopsins in retinal neurons with subcellular targeting motifs: for the study of the structure/function of aii amacrine cells and for vision restoration

Chaowen Wu
Wayne State University,

EXPRESSION OF MICROBIAL RHODOPSINS IN RETINAL NEURONS WITH SUBCELLULAR TARGETING MOTIFS: FOR THE STUDY OF THE STRUCTURE/FUNCTION OF AII AMACRINE CELLS AND FOR VISION RESTORATION

by

CHAOWEN WU

DISSERTATION

Submitted to the Graduate School

of Wayne State University,

Detroit, Michigan

in partial fulfillment of the requirements

for the degree of

DOCTOR OF PHILOSOPHY

2011

MAJOR: ANATOMY & CELL BIOLOGY

Approved by:

_____

Advisor Date

_____

_____

_____

ACKNOWLEDGEMENTS

First and foremost, I want to thank my advisor Dr. Zhuo-Hua Pan for fostering a lab environment that is always filled with interesting ideas and great people. Your guidance helped me grow into an independent and confident scientist. I would like to thank my dissertation committee members: Dr. Dennis Goebel for your kind encouragement and being so generous with your time, Dr. Paul Walker for challenging me and strengthening my critical thinking, and Dr. Jianjun Wang for never hesitating to tell me the truth and always pushing me to reach my potential.

I would also like to thank my colleagues Dr. Elena Ivanova for passing your vast knowledge to me and Dr. Jinjuan Cui, Qi Lu, and Tushar Ganjawala for all the valuable help you have been for me.

Last but not least, I want to thank my mother, Zhongyi Huang, and my father, Dr. Shezhang Wu for your unconditional support and for instilling in me the value of education. And of course, I want to thank my sister, Dr. Yanwen Wu, for being the voice of /pyeh.

TABLE OF CONTENTS

LIST OF TABLES

LIST OF FIGURES

CHAPTER 1

BACKGROUND AND RATIONALE

The retina is a neural tissue composed of an intricate and complex interconnection of neurons functioning together to encode light signals for visual perception. Gaining knowledge about the structure and function of retinal neurons would not only improve our understanding of the visual circuitry, it would also have implications for how we can use this knowledge in potential therapies in the treatment of blindness. One such tool that could aid in both pursuits is the protein targeting motif.

In order for cells to function properly, newly synthesized proteins must be delivered to the correct location to serve their specialized function. For example, in the neuron, the clustering of Na^+ channels at the axon initial segment is important for mediating action potential generation (Kole et al., 2008). The peptide signals responsible for protein targeting were discovered by Günter Blobel who found that proper subcellular localization of proteins was dictated by short intrinsic regions of the amino acid chain (Blobel et al., 1979; Lingappa et al., 1980; Blobel, 1980). Such regions, or targeting motifs, serve as addresses to direct intracellular trafficking machinery to transport newly synthesized proteins to their proper final location. In this

dissertation, Chapters 2 will discuss how targeting motifs can be used to increase our fundamental understanding of neuron morphology, specifically of the AII amacrine cell, and Chapter 3 will discuss how targeting motifs can be used to manipulate retinal ganglion cell (RGC) receptive field as a strategy to improve a technique for vision restoration.

Using targeting motifs to study basic neuronal structure and function

The vertebrate retina has three main cell layers. The most distal layer is called the outer nuclear layer (ONL) containing cell bodies of the light sensing photoreceptors (rods and cones). The center layer is called the inner nuclear layer (INL) mainly containing cell bodies of bipolar cells, horizontal cells, and amacrine cells. The most proximal layer is called the ganglion cell layer (GCL) mainly containing cell bodies of retinal ganglion cells (RGCs). In the vertical and excitatory flow of information, photons are absorbed at the light sensing photoreceptors whose axonal processes synapse onto bipolar cell dendrites in the outer plexiform layer (OPL). Bipolar cell axon terminals then synapse onto RGC dendrites in the inner plexiform layer (IPL). RGC axons form the optic nerve which exits the retina and relays light information to the brain. Interspersed between the vertical

excitatory connections are the inhibitory interneurons. Horizontal cells mediate inhibitory interactions in the OPL connections while amacrine cells mediate inhibitory interactions in the IPL. The knowledge about photoreceptors, bipolar cells, RGCs, horizontal cells, amacrine cells, and major neuron sub-types have been gained through microscopy and published in 1900 in the works of Santiago Ramón y Cajal. Since then, numerous sub-types with less obvious morphological distinctions have been classified owing to new tools that have allowed for the study of individual neurons at levels of detail that could not have been resolved under a light microscope (Reviewed in Masland, 2001).

Illuminating retinal cell types

Fluorescence tagging and labeling have added to the ability to visualize retinal neuron morphology. It is especially advantageous in the compact environment of the retina to be able to label specific populations of neurons or individual neurons. Techniques used in our lab for this purpose include antibody labeling and chemical or viral mediated fluorescence protein expression. Previous work in the lab found by injecting adeno-associated virus 2/2 (AAV2/2) carrying the gene for green fluorescence protein (GFP) into the eye, select retinal cell populations can be illuminated following GFP expression (Bi et al., 2006). One population that is of interest is the AII amacrine cell which

was found to be preferentially transduced by low concentration AAV2/2 injection (Ivanova and Pan, 2009).

The AII amacrine cell

The AII amacrine cell is an axonless glycinergic (Pourcho and Goebel, 1985; Crooks and Kolb, 1992) interneuron in the mammalian retina originally known for its crucial role in mediating scotopic (night-time) vision (Famiglietti et al., 1975) and recently also for its involvement in detecting approaching objects in photopic (day-time) vision (Münch et al., 2009). The cell is conventionally depicted as a bistratified neuron with two distinct dendritic trees: the distal dendrites (arboreal dendrites) terminate in the retinal inner plexiform layer (IPL) ON-sublamina, and the proximal dendrites (lobular appendages) terminate in the OFF-sublamina. AII amacrine cells pass rod signals from rod bipolar cells received through the arboreal dendrites to the ON cone pathway at the arboreal dendrites, and to the OFF cone pathway at the lobular appendages (Bloomfield and Dacheux, 2001) (Figure 1). Although it is believed that AII amacrine cells primarily use graded potentials for information processing, accumulating evidence suggests that action potentials or spikes play an important role (Boos et al., 1994; Veruki and Hartveit, 2002a; Veruki and Hartveit, 2002b; Tamalu and Watanabe, 2007; Tian et al., 2010). Na^+ channel-

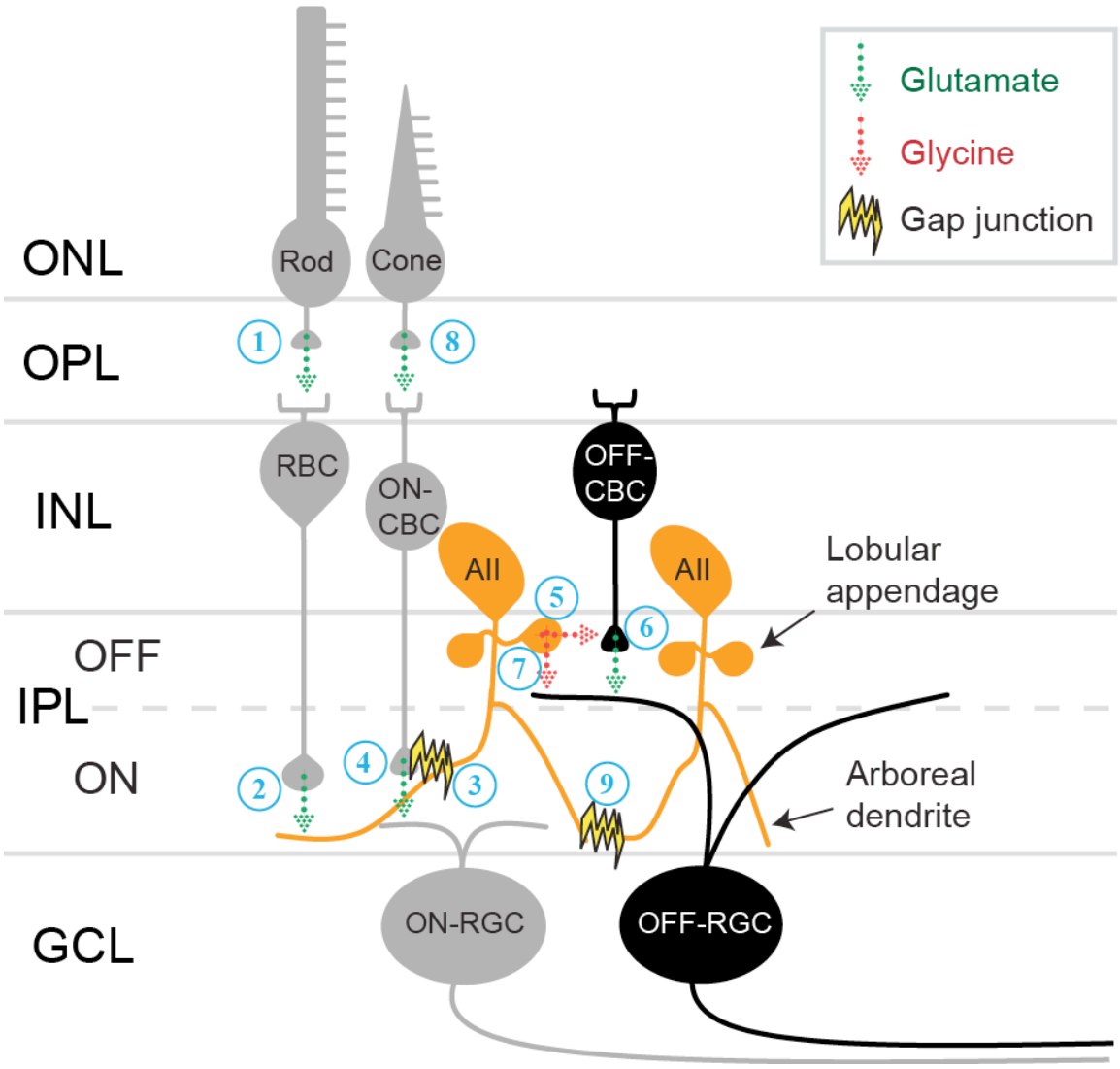

Figure 1: AII amacrine cell circuits. 1. In scotopic vision, rods sense light and excite RBCs. 2-3. RBCs synapse onto AII arboreal dendrites that excite ON-CBCs through gap junctions. 4. ON-CBCs excite ON-RGCs. 5-7. At the same time, AII lobular appendages inhibit OFF-CBC glutamate release onto OFF-RGCs and directly inhibit OFF-RGCs with glycine. Therefore, excitation of AIIs leads to excitation of ON-pathways and inhibition of OFF-pathways. 8. In photopic vision, cones sense light and excite ON-CBC that may utilize gap junctions in reverse to excite AIIs at the arboreal dendrites leading to inhibition of the OFF-pathway (Münch et al., 2009). 9. Finally, AIIs are electrically coupled through arboreal dendrite gap junctions. *ONL/OPL: outer nuclear/plexiform layer; INL/IPL: inner nuclear/plexiform layer; GCL: ganglion cell layer; RBC/CBC: rod/cone bipolar cell.*

dependent spiking in the AII amacrine cell is well documented (Bloomfield and Xin, 2000; Boos et al., 1993; Tamalu and Watanabe, 2007). Studies have suggested that Na^+ channels are likely located close to the proximal dendrites (Tamalu and Watanabe, 2007), but the precise location and the nature of spike origin has remained elusive.

Targeting motif mediated study of AII amacrine cell structure and function

In order for proteins to serve their correct function in a cell, they must be transported to the proper subcellular location. One important group of proteins that must be precisely targeted to their destination are voltage-gated ion channels. Voltage-gated ion channels play a main role in modulating the excitability and kinetics of a neuron, specifically in action potential generation. Ion channels including voltage-gated Na^+ channels (Navs) are found clustered at the site of action potential spike initiation called the axon initial segment (AIS) (Boiko et al., 2003; Garrido et al., 2003). The AIS is located in the proximal axon near the soma. Therefore in axon-bearing spiking neurons, action potentials typically have a predictable site of initiation. However in axon-less spiking neurons, such as the mammalian retinal AII amacrine cell, the site of spike initiation is less predictable therefore requires additional investigation.

Based on the idea that action potential generation requires the clustering of voltage-gated Na^+ channels (Kole et al, 2008), following the intracellular transport of Navs should lead to the site of spike initiation. Therefore to localize Navs within the AII amacrine cell, a Nav-targeting motif was linked to GFP. The results of AAV2/2-mediated expression of Nav-motif targeted GFP are discussed in Chapter 2.

Using targeting motifs to improve current strategies in vision restoration

Targeting-motifs can also be applied as a tool in vision restoration. The progressive loss of photoreceptor cells in many human retinal degenerative diseases, such as retinitis pigmentosa, results in partial vision loss or complete blindness. Since photoreceptors do not regenerate in the mammal after birth, our lab sought to restore vision by genetically converting the surviving inner retinal neurons, specifically RGCs, into photosensitive cells, thus imparting light-sensitivity to retinas deficient in photoreceptors (Bi et al., 2006).

Light activated microbial rhodopsins for vision restoration therapy

The critical component of the strategy is to convert RGCs into directly light-sensitive cells, therefore act as the new photoreceptors. This can be achieved through the insertion of light-activated

membrane proteins, channelrhodopsin-2 (ChR2) or Halorhodopsin (NpHR), into the RGC membrane.

ChR2 is a microbial rhodopsin cloned from the green algae, C*hlamydomonas reinhardtii* (Sineshchekov et al., 2002; Nagel et al., 2003; Suzuki et al., 2003). There are several differences between microbial rhodopsin and animal rhodopsin. Animal rhodopsin found in photoreceptors uses an 11-*cis* isomer of retinal as the chromophore for the initial active state. Light causes an 11-*cis* to all-*trans* isomerization which then requires a sequence of changes involving the pigment epithelial cells to recharge the all-*trans* retinal back to the active state (Baylor, 1996; Stryer, 1986; Thompson and Gal, 2003). Furthermore, animal rhodopsin requires coupling between light activation and the regulation of ion movement through the cell membrane via a complex G-protein mediated cascade. In contrast, ChR2 offers a simpler light receptor system. First, ChR2 uses the all-*trans* isomer of retinal as the chromophore, a molecule that is believed to be ubiquitously present in all cells (Thompson and Gal, 2003; Kim et al., 1992). Second, after the all-*trans* retinal undergoes isomerization by light, it is recharged without leaving the opsin-retinal complex. Third, when ChR2 is activated by light, the channel itself is directly involved in the transportation of ions through the membrane (Lanyi and Lueke, 2001; Bamann et al., 2008).

ChR2 is rapidly activated and inactivated by light in the visible range, with action spectrum peak at ~470 nm (Bi et al, 2006; Nagel et al., 2003; Bamann et al., 2008; Boyden et al., 2005; Ishizuka et al., 2006; Li et al., 2005). Additionally, ChR2 can function without further intervention after expression since all-*trans* retinal is ubiquitously present and ChR2 has been shown to produce light-gated conductance with selective permeability to cations, mainly Na^+ and Ca^{2+} (Nagel et al., 2003). This permeability to physiologically relevant cations underlying membrane excitability of retinal neurons, makes ChR2 particularly suitable for the purpose of restoring light sensitivity back in the photoreceptor degenerated retina.

The counterpart to ChR2 is the light-driven chloride pump, NpHR, cloned from *Natronobacterium pharaonis* with peak action spectrum ~570 nm (Lanyi, 1986). In contrast to the depolarizing actions of ChR2, the inward pumping of chloride ions by NpHR results in cell hyperpolarization (Han and Boyden, 2007; Zhang et al., 2007; Zhang et al., 2009).

Feasibility of microbial rhodopsin based therapy

Previous experiments in the lab have demonstrated the feasibility of microbial rhodopsin-based therapy for potential vision restoration. Viral-mediated expression of microbial rhodopsins in RGCs

have been shown to be stable and long-lasting (Bi et al., 2006; Zhang et al., 2009). In whole-cell patch-clamp recordings of RGCs expressing ChR2, light-evoked currents with light intensity-dependent magnitudes were observed. Detectable currents were recorded in most cells at a light intensity of $2.2x10^{15}$ photons cm^{-2} s^{-1}. Membrane depolarization and spike rates were also dependent on light intensity. Specifically, higher light intensity markedly accelerated the voltage response kinetics (Bi et al., 2006). These light-induced responses of ChR2-expressing RGCs are similar to the ON responses produced in normal ON-type RGCs to light increment.

Similarly, NpHR-mediated membrane hyperpolarizations and suppression of spiking activity can be triggered rapidly in RGCs at light intensity $>10^{16}$ photons $cm^{-2}s^{-1}$. Furthermore, after light stimulus termination, rapid robust rebound activity can also be observed (Zhang et al., 2009). These light-induced responses of NpHR-expressing RGCs are similar to the OFF light response produced in normal OFF-type RGCs.

Light responses produced by microbial rhodopsin activation can be recorded as visual evoked potentials (VEPs) in the visual cortex demonstrating that restored light responses from the RGCs can be relayed to the brain.

It was later shown by behavioral works of other laboratories that photoreceptor degenerative mice expressing ChR2 in their ON-bipolar cells through electroporation appeared to be able to distinguish a light from a dark environment. Furthermore, these mice are able to display optokinetic responses to rotating vertical bars of light (Lagali et al., 2008). In another study, optokinetic responses were also shown to be restored by expressing ChR2 in RGCs (Tomita et al., 2010). These results provided additional support that ChR2 gene therapy could be a feasible way to restore light perception. However in another study that tested behavior in mice expressing ChR2 only in RGCs driven by the *Thy1* promoter, these mice did not perform better than their untreated counterparts (Thyagarajan et al., 2010). The behavioral discrepancy reported in these two studies between restoration of light response at the bipolar cell level versus at the RGC level may allude to the importance of information attained through intra-retinal processing.

Center-surround opponency of RGCs

The normal processing of light into perceived vision begins at the photoreceptors that initiate a cascade of signaling through the three retinal cell layers and exits the retina via RGC axons that form the optic nerve. Various features of the visual world is extracted through this intraretinal processing including color, luminance, edges, and

motion (Cleland and Levick, 1974; DeVries and Baylor,1997). Expression of ChR2 or NpHR alone can impart the function of luminance detection to RGCs, however by bypassing intraretinal processing pathways, certain levels of information about the visual scene will be lost. One important piece of information is the representation of edges. Edge detection is a consequence of intraretinal processing that ultimately creates a center-surround receptive field in the RGC.

The center-surround is organized into a smaller center receptive field and a larger encompassing surround receptive field that mutually oppose each other. The surround inhibition is thought to be mediated by horizontal cells (Naka, 1971; Mangel, 1991) and amacrine cells (Taylor 1999; Van Wyk et al., 2009). In the ON-center RGC, light in the receptive field center activates the neuron while light in the receptive field surround inhibits the neuron. Conversely in the OFF-center RGC, dimming of light in the receptive field center activates the neuron while dimming in the receptive field surround inhibits the neuron (Kuffler, 1953). The opposing actions of center-surround enhances neuron activity at stimuli edges when the center and surround receptive field areas are heterogeneously lit. This is in contrast to the uniform receptive field that would be created by ChR2 expression alone in the RGC which would activate the neuron not only

at the edge of a light stimulus, but to an even greater extent when the receptive field is homogeneously lit. Therefore it would be advantageous to restore a center-surround receptive field in the RGC for the purpose of enhancing edge detection. This can theoretically be accomplished by differentially targeting ChR2 and NpHR to the center or surround regions of the RGC dendritic field using targeting-motifs to establish regions of opposing actions to light stimulation.

Targeting-motif mediated center-surround receptive field in the RGC

The normal receptive field center is approximately the size of the RGC dendritic field while the receptive field surround is approximately 3-5 times wider due to interactions with upstream neurons. Since microbial rhodopsin therapy renders an RGC directly light sensitive, recreating a center-surround receptive field directly in an RGC limits the receptive field to the size of the dendritic field. Therefore in order to create a smaller center with a larger encompassing surround, subcelluar targeting would be required. For this reason, targeting motifs with preferential subcellular distributions were investigated. The results for motif-mediated creation of the center-surround receptive field in RGCs are discussed in Chapter 3.

CHAPTER 2

Action potential generation at an AIS-like process in the axonless retinal AII amacrine cell

SUMMARY

In axon-bearing neurons, action potential spikes conventionally initiate at the axon initial segment (AIS) and are important for neuron excitability and cell-to-cell communication. However in axonless neurons, spike origin has remained unclear. This study reports in the axonless spiking AII amacrine cell of the mammalian retina a dendritic process sharing organizational and functional similarities with the AIS. This process was revealed through viral-mediated expression of channelrhodopsin-2-GFP (ChR2-GFP) with the AIS-targeting motif of sodium channels (NavII-III). AII-processes showed clustering of voltage-gated Na^+ channel 1.1 (Nav1.1) as well as AIS markers ankyrin-G and neurofascin. Furthermore, NavII-III targeting disrupted Nav1.1 clustering in the AII-process which drastically decreased Na^+ current and abolished the ability of the AII amacrine cell to generate spiking. These findings indicate that despite lacking an axon, spiking in the axonless neuron could originate at a specialized AIS-like process.

INTRODUCTION

Sites of action potential generation have been implicated as important sources of neuronal plasticity and optimization of neuronal signaling (Kuba et al., 2006; Kuba et al., 2010; Grubb and Burrone, 2010; Losonczy et al., 2008). Although it is known that action potentials typically initiate at the AIS in axon-bearing neurons (Coombs et al., 1957; Palmer and Stuart, 2006; Kole et al., 2008), is not known where action potentials are produced in axonless neurons. To address this question, the site of action potential generation was investigated in the axonless spiking AII amacrine cell.

In this study took advantage of the AII amacrine cell's own protein trafficking machinery to investigate the spike initiation site within this axonless neuron. Spike generation at the AIS requires voltage-gated Na^+ (Nav) channel clustering (Kole et al., 2008). Nav1 subunits share a conserved amino acid motif (NavII-III) shown to be necessary and sufficient to target proteins to the AIS (Garrido et al., 2003; Lemaillet et al., 2003). By linking NavII-III to ChR2 for membrane anchoring, and green fluorescent protein (GFP) for visualization, ChR2-GFP-NavII-III expression in the AII amacrine cell revealed an AIS-like compartment within its dendritic trees. This

suggests that axonless neurons could possess similar compartmental organization as axon-bearing neurons for action potential generation.

METHODS

DNA and viral vector construction

Adeno-associated virus serotype 2 (AAV2/2) cassette carrying the channelrhodopsin-2 and GFP (ChR2-GFP) fusion construct (Bi et al., 2006) was modified by inserting the 27 amino acid ankyrin binding domain from Nav1.6 (NavII-III: 5’ - TVRVPIAVGESDFENLNTEDVSS ESDP - 3’) (Garrido et al., 2003) at the 3’ end of GFP. ChR2-GFP-NavII-III vector with CAG (a hybrid CMV early enhancer/chicken B-actin) promoter was packaged and affinity purified at the Gene Transfer Vector Core of the University of Iowa.

Animals and AAV2/2 vector injection

All animal experiments and procedures were approved by the Institutional Animal Care Committee at Wayne State University, and were in accord with the NIH Guide for the Care and Use of Laboratory Animals. Adult C57BL/6J mice aged 1–2 months were used for virus injections. Animals were anesthetized by intraperitoneal injection of ketamine (120 mg/kg) and xylazine (15 mg/kg). Under a dissection

microscope, 1.0 µl of viral vector suspension was injected into the intravitreal space of each eye using a Hamilton syringe with a 32-gauge blunt-ended needle. Three groups of animals were injected. The motif-targeted group received injections of AAV2/2-ChR2-GFP-NavII-III at two different concentrations of 5 $x10^{10}$ GP/ml and 3-13$x10^{12}$ GP/ml for histology/immunohistochemistry and patch-clamp recordings, respectively. The injected-control group received injections of AAV2/2-ChR2-GFP at 4 $x10^{12}$ GP/ml. The uninjected-control group did not receive any injections. Animals were used for experiments at least one month after viral injection.

Histology/immunohistochemistry

Animals were sacrificed by CO_2 asphyxiation followed by decapitation and enucleation for experiments. Enucleated eyes were fixed in 4% paraformaldehyde in phosphate buffer (PB) at room temperature (RT) for 20 minutes. GFP-expression was examined in flat-mounted retinas and vertical sections. For vertical sections, fixed retinas were cryoprotected in a sucrose gradient (10%, 20%, and 30% w/v in PB) and cryosectioned at 20µm thickness. Slides with cryosections were thawed at RT and washed 3x20 min in PB followed by a 40 min incubation in blocking solution that contained 5% Chemiblocker (Chemicon, Temecula, CA), 0.5% Triton X-100, and

0.05% sodium azide. For immunostaining, the following primary antibodies were diluted in blocking solution and applied to sections for overnight RT incubation: mouse anti-ankG (1:20000; Neuromab), rabbit anti-pan-NF (1:2000; Abcam), mouse anti-Nav1.1 (1:4000; Neuromab), rabbit anti-SPo (1:60000; Synaptic Systems), and mouse anti-GlyRα1 (1:4000; Synaptic Systems). The next day, slides were washed 3x20 min in PB and secondary antibodies diluted in blocking solution was applied for a 1 h RT incubation in the dark. Slides were then washed 3x20 min in PB and mounted in Vectashield (Vector Laboratories) for fluorescence microscopy. All images were acquired using a Zeiss Axioplan 2 microscope with Apotome (Carl Zeiss) with the AxioVision software. Z-stack images were taken at optical sections of 0.6 µm apart. Brightness and contrast was adjusted with Adobe Photoshop CS5 (Adobe Systems).

Patch-clamp recordings *(performed in collaboration with Dr. Elena Ivanova and Dr. Jinjuan Cui)*

Retinal slices were prepared as previously described (Ivanova and Pan, 2009). Whole-cell patch-clamp recordings in control were performed in oxygenized HANKS solution (in mM): NaCl, 136.8; KCl, 5.4; KH2PO4, 0.4; NaH2PO4, 0.3; CaCl2, 1.3; MgCl2, 0.5; MgSO4, 0.5; HEPES, 5.0; D-Glucose, 22.0; phenol red 0.03; pH 7.2. The intracellular solution

contained (in mM): K-gluconate, 140.0; KCl, 7; EGTA, 0.1; MgCl2, 4.0; HEPES, 10; NaATP, 2.0; NaGTP, 0.5; Alexa568 hydrozide sodium salt (Molecular Probes, Eugene, OR), 0.1; pH 7.4. The blockade of spontaneous activity in voltage clamp was assessed by the addition of tetrodotoxin (TTX) (1 μM) or 6-Cyano-7-nitroquinoxaline-2,3-dione (CNQX) (15 μM); or the combination of CNQX with strychnine (1 μM) and picrotoxinin (50 μM) to HANKS. The recordings of current injection evoked spike activity were performed in HANKS with CNQX (15 μM), strychnine (1 μM), and picrotoxinin (50 μM). To examine voltage-gated Na+ current we used HANKS with (in mM) CdCl2 0.1; tetraethylammonium chloride (TEA) 10; CNQX 15; strychnine 1; picrotoxinin 50. Intracellular solution was (in mM): Cs-acetate, 130.0; TEA-Cl, 10; EGTA, 0.1; MgCl2, 4.0; HEPES, 10; NaATP, 2.0; NaGTP, 0.5; Alexa568, 0.1; pH 7.4. In all experiments 1 μM tetrodotoxin was applied to block Na+ current. All chemicals were purchased from Sigma-Aldrich (St. Louis, MO). Liquid junction potential (~10 mV) was corrected. The resistance of the electrode was ~8 MΩ. Pipette and cell capacitances were canceled. Data were analyzed off-line using the ORIGIN (Microcal Software, Northampton, MA) program. ChR2-mediated light responses were evoked by a 300 W xenon-based lamp (Lambda LS, Sutter Instrument, Novato, CA) that was coupled to the microscope with an optical fiber. A band-pass filter of 420-490 nm was

used to optimize the light spectrum (Nicon B-3A filter). The light intensity that elicited ChR2 responses was 8.2 x 1018 photons cm-2s-1.

RESULTS

Viral-mediated NavII-III-targeted expression in the retina

In vivo expression of ChR2-GFP-NavII-III in the mouse retina was achieved through AAV2/2-mediated gene delivery by intravitreal injection (Bi et al., 2006). As expected, ChR2-GFP-NavII-III expression in the RGC was concentrated in the AIS (Figure 2a: arrowheads). In addition, GFP fluorescence was also brightly concentrated in smaller processes throughout the inner plexiform layer (IPL; Figure 2a arrows). These processes were suspected to belong to AII amacrine cells due to the high tropism of AAV2/2 for AIIs (Ivanova and Pan, 2009). Indeed in vertical section, each process was found to originate from one AII amacrine cell at the lobular appendages (AII-process). AII-processes were varied in orientation, conformation, and terminated in both ON- and OFF-sublaminae of the IPL and occasionally in the inner nuclear layer (INL) (Figure 2b).

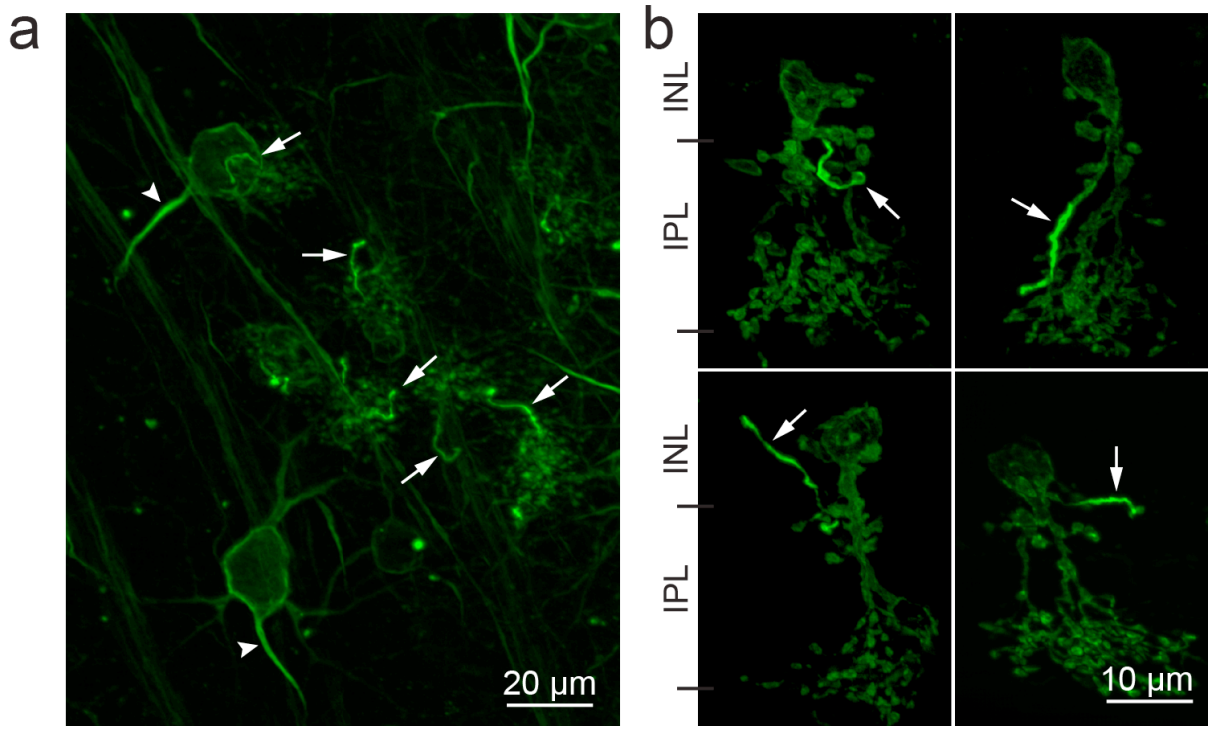

Figure 2: ChR2-GFP-NavII-III expression in the retina. **(a)** In retinal flat-mount, NavII-III expression was concentrated in RGC AIS (arrowheads) and smaller processes (arrows) suspected to belong to AIIs. **(b)** In retinal vertical section, each AII was observed with one NavII-III targeted process (arrows) of varying direction and conformation originating from the lobular appendages and terminating in both IPL ON- and OFF-sublaminae and the INL.

Immunohistochemical staining of AIS associated proteins in AII-processes

Because NavII-III is an AIS-targeting motif, the AII-processes was first examined with immunohistochemical (IHC) staining for proteins typically enriched at the AIS. NavII-III contains an ankyrin binding domain which binds the cytoskeletal scaffold protein ankyrin-G (ankG) at the AIS (Garrido et al., 2003; Lemaillet et al., 2003). In vertical sections, ankG immunostaining colocalized with AII-processes (Figure 3a). Similarly, pan-neurofascin (pan-NF) immunostaining against an axonal cell adhesion molecule that functions in the organization of the AIS (Sherman et al., 2005; Hedstrom et al,. 2007) also colocalized with AII-processes (Figure 3b).

Since voltage-gated sodium channels cluster at the AIS and *in situ* hybridization studies have shown AII amacrine cells to express the Nav1.1 subunit (Kaneko and Watanabe, 2007), every AII-process was anticipated to immunostain positively for Nav1.1. However, Nav1.1 immunostaining produced a spectrum of results in retinas infected with a low virus concentration (see Methods). Certain AII-processes stained positively for Nav1.1 (Figure 4a), while others appeared virtually unstained (Figure 4b). There seemed to be an inverse relationship between Nav1.1 staining intensity and GFP fluorescence intensity in the AII-processes. These results implied that targeted expression of

ChR2-GFP-NavII-III may be in competition with endogenous Nav1.1 for ankG binding.

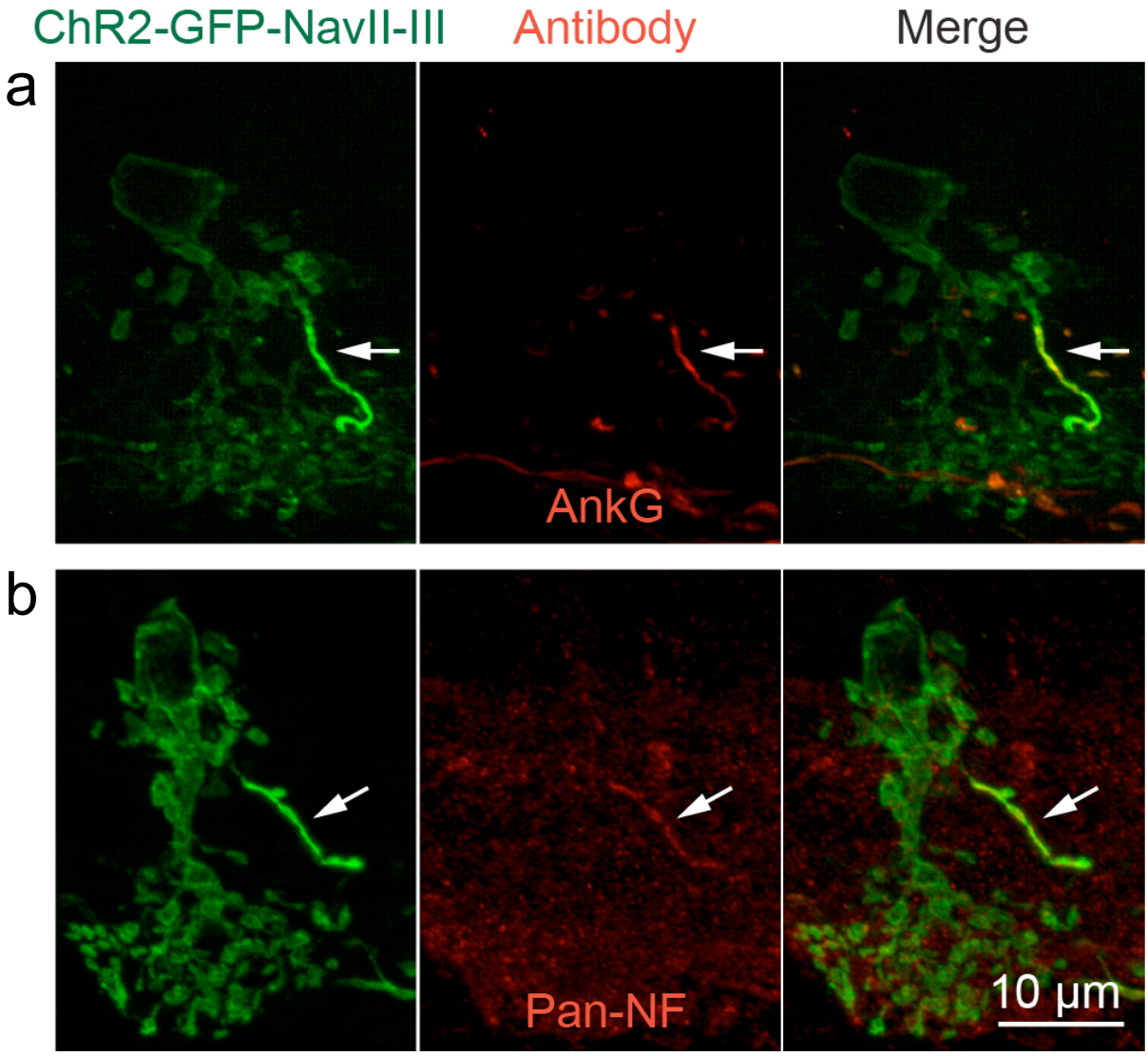

Figure 3: IHC characterization of AIS markers in NavII-III targeted AII-processes. a, b: In AIIs expressing ChR2-GFP-NavII-III, AII-processes colocalized with the AIS markers **(a)** ankG and **(b)** pan-NF.

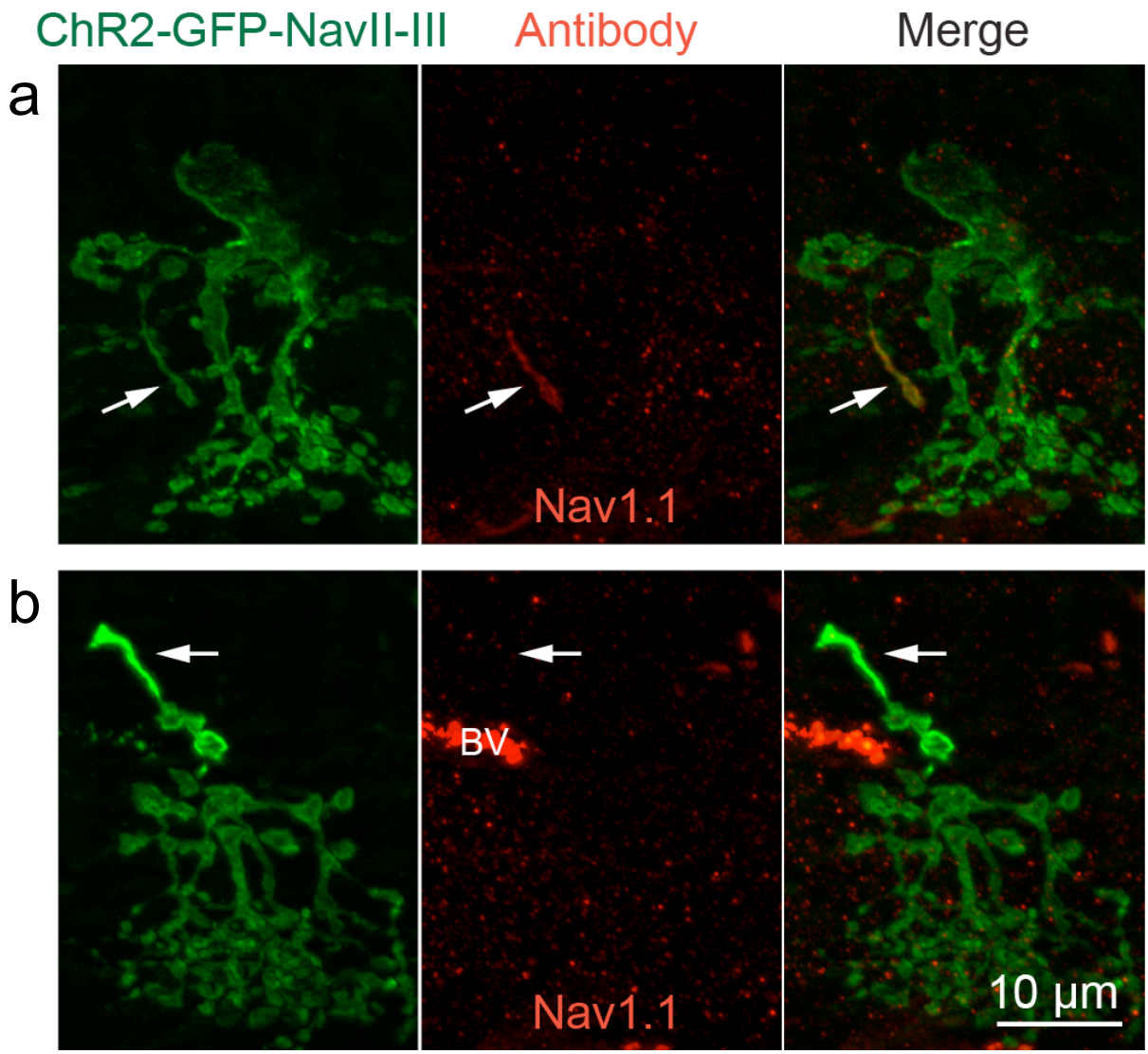

Figure 4: IHC characterization of Nav1.1 in NavII-III targeted AII-processes. **a, b: (a)** In weakly targeted AII-processes, Nav1.1 colocalizaion was observed. **(b)** However in strongly targeted AII-processes, Nav1.1 colocalization was not seen. BV: blood vessel.

IHC of lobular appendage associated elements in AII-processes

AII-processes have AIS features, yet they still resemble lobular appendages particularly at the distal ends where lobules are often formed. To explore this relationship, retinal vertical sections were immunostained for the major synaptic vesicle protein found in lobular appendages, synaptoporin (SPo) (Brandstätter et al., 1996). In vertical sections, 97% (n = 58) of AII-processes examined colocalized with SPo immunostaining (Figure 5a). To investigate whether AII-processes potentially had a postsynaptic partner, retinal vertical sections were immunostained with antibodies against the glycine receptor α1 subunit (GlyRα1) postsynaptic to lobular appendages (Sassoe-Pognetto et al., 1994; Grünert and Wässle, 1996). When NavII-III expressing AII-processes were examined, 84% (n = 45) appeared to colocalize with GlyRα1 puncta (Figure 5b: GlyRα1). These results suggest that AII-processes likely contain the sites of presynaptic glycine release.

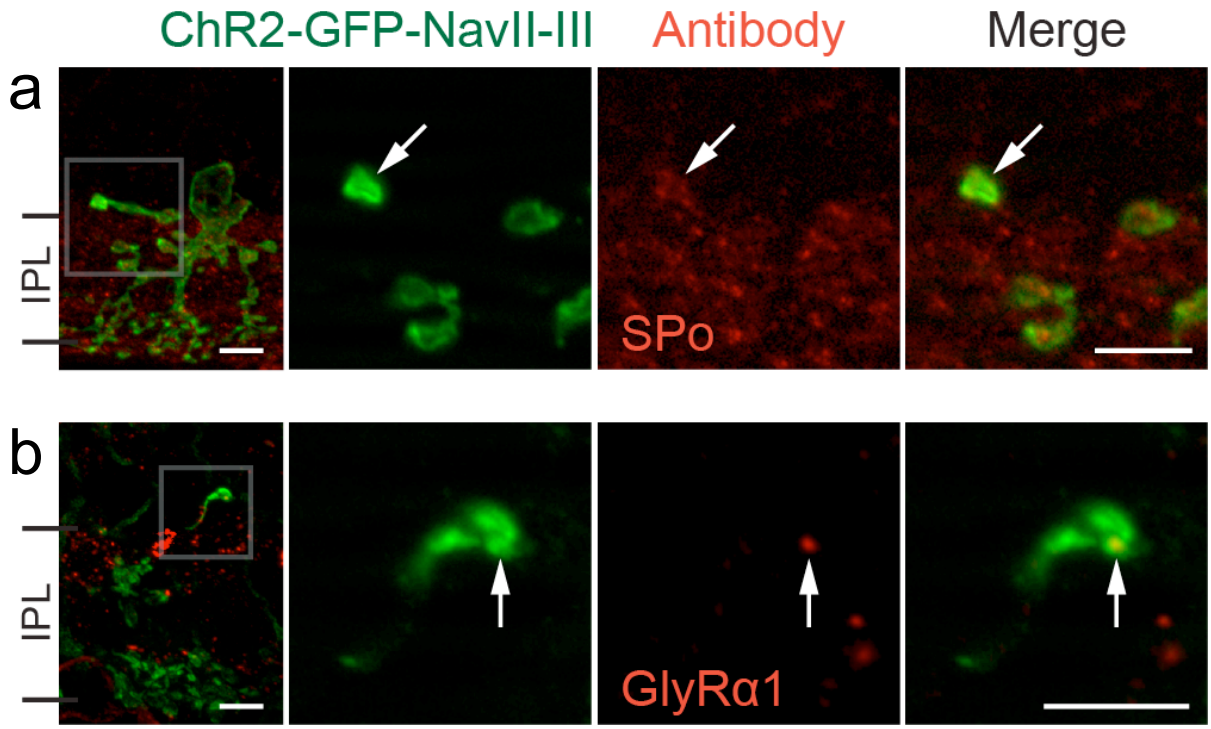

Figure 5: IHC characterization of lobular appendage features in AII-processes. a, b: The first panels are z-stack projections and three subsequent panels are single plane magnifications of the corresponding boxed areas showing an AII-process terminal colocalizing with **(a)** SPo immunostaining and **(b)** an AII process colocalizing with a GlyRα1 punctum. All scale bars are 5 μm.

Patch-clamp characterization of NavII-III-targeting on AII amacrine cell spiking *(completed in collaboration with colleagues Dr. Elena Ivanova and Dr. Jinjuan Cui)*

Because the expression of ChR2-GFP-NavII-III appeared to disrupt endogenous Nav1.1 clustering in AII-processes, followup experiments carried out in the lab examined this effect on the spiking ability of AII amacrine cells by performing whole-cell patch-clamp recordings in retinal slices. As a control, GFP-labeled AII amacrine cells from eyes injected with virus carrying ChR2-GFP without the NavII-III motif were recorded. In voltage-clamp, the cells frequently displayed large, discrete spontaneous activities (13 out of 29) which were most prominent at holding potential around -60 mV (Figure 6a). These properties were similar to AII amacrine cells recorded from un-injected eyes (13 Out of 24; data not shown). Consistent with previous reports (Boos et al., 1993; Tamalu and Watanabe, 2007), the large spontaneous activities were mediated by voltage-gated Na^+ channels because they were blocked by tetrodotoxin (TTX) (Figure 6b; n= 3). The presence of Na^+ current is likely due to the inability to achieve adequate space-clamp in AII amacrine cells (Boos et al., 1993; Tian et al., 2010) In addition, there were often many small spontaneous activities which were insensitive to TTX but were blocked by glutamate antagonists, CNQX or the combination of the CNQX, GABA and glycine

receptor antagonists (Figure 6b; n =7), indicating that these were excitatory or inhibitory postsynaptic currents. In contrast to the control, no TTX-sensitive spontaneous activities were observed in any AII amacrine cells expressing ChR2-GFP-NavII-III (Figure 6c; n = 21). For every cell recorded in both groups, the functional expression of ChR2 was confirmed by the ChR2-mediated light responses (Figure 6d and e). These results indicate that AII amacrine cells with NavII-III motif targeted expression of ChR2-GFP lost the Na^+ channel-mediated spontaneous activity.

Next, spiking activity evoked by current injection in current-clamp with the suppression of all synaptic inputs was examined. Spiking activity was evoked in the majority of recorded AIIs expressing ChR2-GFP without motif (11 out of 13; Figure 6f). Spike frequency increased with the increase of injected current as previously reported (Tamalu and Watanabe, 2007). Again, no spiking activity was observed in any of the recorded AII amacrine cells in the NavII-III targeted group (n = 7; Figure 6g). Finally, voltage-gated Na^+ current between control and NavII-III targeted groups were compared. The recordings were made under the condition that all other voltage-gated currents and neurotransmitter-activated receptors were blocked to isolate Na^+ currents. Na^+ currents were observed in the majority of recorded AII amacrine cells in the control group (5 out of 7; Figure 6h) but barely

detected in the majority of the NavII-III targeted group (Figure 6i top panel). Only in a few cells (3 out of 13) were Na^+ currents observed (Figure 6i bottom panel). The average peak current for the control group (84.3 ± 24.7 SEM; n = 7) was significantly different from that of the NavII-III targeted group (6.4 ± 4.3 SEM; n = 13; two-tailed t-test, $P < 0.001$; Figure 6j). Together, these results indicate that targeted ChR2-GFP-NavII-III expression largely abolished Na^+ currents along with the spiking ability of AII amacrine cells.

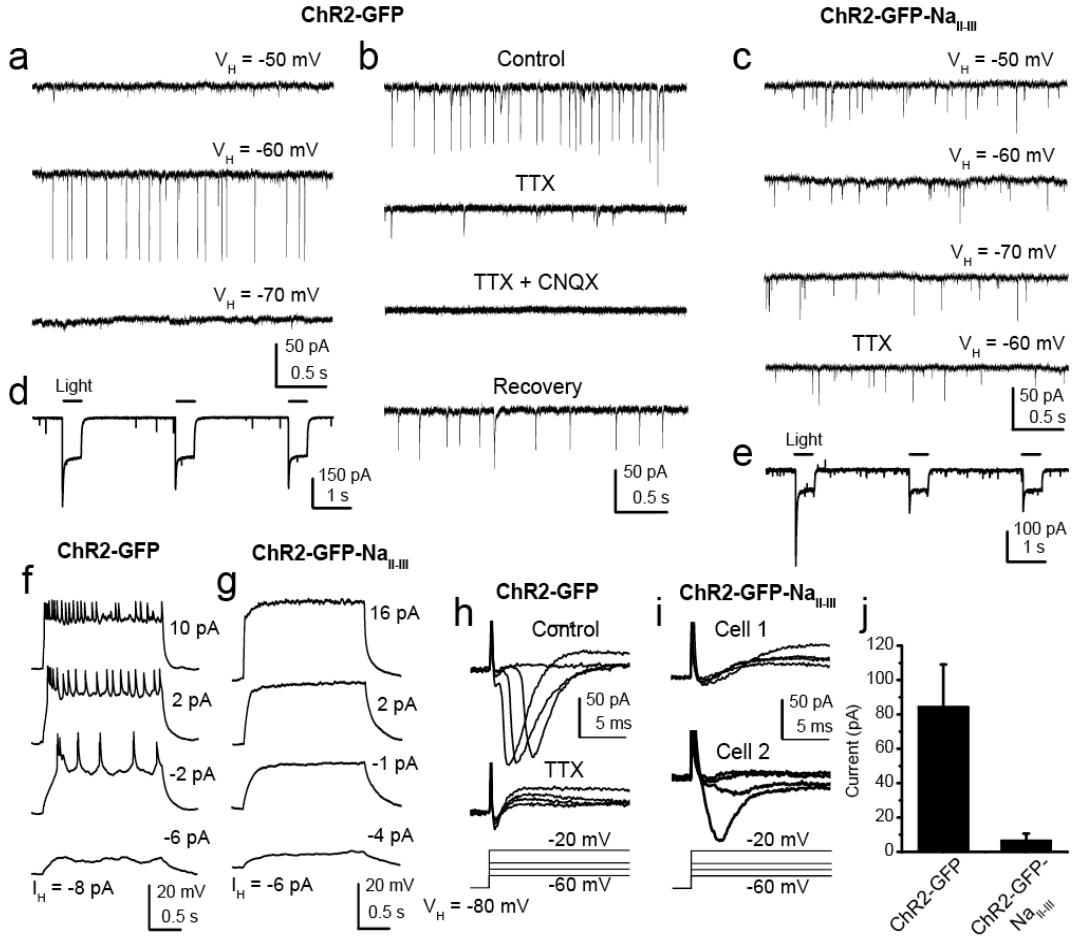

Figure 6: Patch-clamp recordings of Na^+ channel-mediated spiking activity and Na^+ current in AIIs. **a, b: (a)** Spontaneous activities of an AII in the control group at three different holding potentials (-50 mV, -60 mV, and -70 mV). **(b)** The activities were blocked by TTX; the remaining spontaneous activities were abolished by TTX + CNQX. Membrane potential was held at -60 mV. **(c)** Spontaneous activities of an AII in the NavII-III targeted group at three different holding potentials (-50 mV, -60 mV, and -70 mV). The activities were not sensitive to TTX blockade (bottom trace). **d, e:** ChR2-mediated light responses for the cells shown in (a) and (c), respectively. **f, g: (f)** Depolarizing current injections from ~-80 mV elicited spikes in an AII in the control group **(g)** but not in the NavII-III targeted group. **h, i:** Na^+ currents activated by depolarization of AIIs from -80 mV to indicated voltages (upper panels). **(h)** A representative recording from a cell in the control group. The current was blocked by TTX (1 μM). **(i)** Recordings from the NavII-III targeted group of a cell with no Na^+ current (top) and a cell with the largest Na^+ current (bottom). **(j)** Average peak Na^+ currents for the control and the NavII-III targeted groups.

DISCUSSION

This study demonstrated that clustering of Na^+ channels at an AIS-like process in the AII amacrine cell is essential for spike generation in this axonless neuron. These AIS-like processes are likely the morphologically distinct processes immuno-labeled by Nav1.1, ankyrin-G and neurofascin reported in the rat retina. However, despite efforts to double label AII amacrine cells with antibodies and Nav1.1, the study was unable to link these processes to their cells of origin (Van Wart et al., 2005). Results from this study thus demonstrate an advantage of motif targeted fluorescent protein expression in identifying this elusive compartment in the AII amacrine cell.

Potential role of action potential generation at an AIS-like process in AII amacrine cells

What might be the functional role of Na^+ channel clustering at this unconventional AIS-like process in the AII amacrine cell? In general, as the case of the AIS, voltage-gated Na^+ channel clustering could facilitate spiking by lowering the threshold of spike generation (Kole et al., 2008). In fact, action potentials mediated by Na^+ channels have been shown to boost the excitatory postsynaptic potentials of AII amacrine cells (Tamalu and Watanabe, 2007; Tian et al., 2010), which

are able to transmit through electrical synapses between AII amacrine cells and to downstream cone bipolar cells (Veruki and Hartveit, 2002a, Veruki and Hartveit, 2002b). Thus, action potentials may function to synchronize the synaptic transmission to ON and OFF cone pathways as well as activity in the AII-network (Veruki and Hartveit, 2002a). It is also plausible that Na^+ channel clustering in the lobular appendages may function to differentially fine tune signal transmission to downstream ON an OFF cone pathways. But surprisingly, a recent study reported that although AII action potentials accelerated the light response to downstream RGCs, blocking voltage-gated Na^+ channels did not differentially affect ON and OFF responses, nor attenuate the response amplitudes of RGCs in scotopic vision (Tian et al., 2010). Since AII action potential generation is membrane potential sensitive, its functional role could be dependent on light adaptation conditions of the retina. With extensive synaptic connectivity with at least twelve different classes of retinal neurons (Anderson et al., 2011) and the range of information processing capabilities from scotopic to photopic vision (Münch et al., 2009; Bloomfield and Dacheux, 2001), it remains to be determined whether AII action potentials could play a role in other information pathways.

Inhibitory amacrine cells have been implicated in contributing to the center-surround receptive-field in RGCs which sharpens the

ganglion cell's spatial tuning and predicted to enhance contrast sensitivity, edge detection, and visual acuity (Münch et al., 2009). Surround inhibition in certain RGCs are created by glycinergic amacrine cells (Van Wyk et al., 2009). Furthermore, blocking amacrine cell spiking with TTX has been shown to reduce surround inhibition in certain RGCs (Taylor, 1999). Localizing the site of spike generation in amacrine cells, such as in the AII amacrine cell, may provide a clue to their potential role in mediating visual discrimination.

AIS-like processes in other neurons?

Considering results showing AII action potentials to significantly speed signaling (Tian et al., 2010), an intriguing hypothesis is that AIS-like processes may be a feature of axonless spiking interneurons involved in fast sensory discrimination. Support for this hypothesis may come from inhibitory interneurons in the olfactory bulb. The olfactory bulb granule cell, another population of axonless spiking inhibitory interneurons, has recently been demonstrated to play a direct role in fast and accurate odor discrimination (Abraham et al., 2010). It would be interesting to determine whether AIS-like processes can be localized within granule cell dendrites. While it is not known what precise advantages are provided by spike generation via an AIS-like process, these data provide a target for further investigations in

the visual system. Furthermore, motif targeting provides a way for visualizing spike generating zones as well as simultaneous disruption of spiking function in neurons. This could offer a potential tool for investigating neuron morphology and function in the olfactory system as well as other regions of the nervous system.

CHAPTER 3

Targeting motif-mediated recreation of the center-surround receptive field in the retinal ganglion cell

SUMMARY

In photoreceptor degenerative diseases such as retinitis pigmentosa, RGC morphology remains largely intact (Mazzoni et al., 2008). One attempt to restore light-sensitivity back in the retina involves the introduction of light-activated microbial rhodopsin (channelrhodopsin-2) into surviving RGCs. RGCs are the output neurons of the retina responsible for relaying processed light information about the visual world to the visual centers of the brain, therefore it would be advantageous to reproduce a key feature of the RGC receptive field: center-surround antagonism. Results of this study showed that a smaller center and a larger encompassing surround receptive field can be generated directly in a single RGC through the use of protein targeting motifs. Resulting morphological dendritic field and physiological response field by center-targeting were significantly smaller than those produced by surround-targeting. Motif-targeting

may be a promising approach in restoring center-surround antagonism in the RGC despite bypassing intraretinal processing.

INTRODUCTION

Center-surround antagonism is an important feature in visual information processing repeated throughout multiple retinal cell types. It is particularly key to RGC physiology characterized by mutual antagonism between concentric center and surround receptive field areas (Hartline, 1938; Hartline, 1940; Kuffler, 1953; Wiesel, 1959; Nelson et al., 1993). This antagonistic center-surround organization is important in providing critical information for the visual processing of enhanced contrast sensitivity (Enroth-Cugell and Robinson, 1966; Shapley and Victor, 1979; Shapley and Victor, 1986; Kaplan and Shapley, 1986) and edge detection (Levick, 1967; Shapley and Tolhurst, 1973; Van Wyk et al., 2006; Russel and Werblin, 2010).

Vision begins in the retina where photoreceptors convert light energy into electrical and chemical signals. These signals are then sent to bipolar cells which synapse onto retinal ganglion cells (RGCs). At the same time, lateral processing by horizontal cells and amacrine cells in the retina generate inhibitory interactions which mediates the formation of a center-surround antagonistic receptive field observed in

nearly all RGCs (Werblin, 1972; Famiglietti and Kolb, 1976; Caldwell and Daw, 1978; Caldwell et al., 1978).

Severe photoreceptor degeneration leads to vision loss or blindness, but neurons of the inner retina including RGCs remain largely intact (Chang et al., 2002; Olshevskaya et al., 2004; Santos et al., 1997; Milam et al., 1998). Light-sensitivity can be restored to the retina by rendering the surviving neurons into directly photosensitive cells. This can be achieved though the expression of exogenous light-activated transmembrane proteins directly in RGCs (Bi et al., 2006; Lagali et al., 2008; Zhang et al., 2009) which include the depolarizing cation channel, channelrhodopsin-2 (ChR2), and the hyperpolarizing chloride pump, halorhodopsin (NpHR).

Past studies have demonstrated the feasibility of using ChR2 and NpHR as a potential approach to vision restoration. ChR2 and NpHR expression has been shown to be widespread and stable when transduced into the retina and have been shown to generate light-driven spiking in the RGCs. These responses have been shown to be transmitted to the visual centers in the brain (Bi et al., 2006); Furthermore, visual reflexes and simple light detection behavior can be elicited in photoreceptor degenerative animals after treatment (Lagali et al., 2008; Tomita et al., 2010). However by directly rendering RGCs photosensitive and bypassing normal intraretinal processing, pathways

that lead to the formation of the center-surround receptive field will be lost. For this reason, this study was aimed at investigating the recreation of center-surround antagonism using select protein-targeting motifs in the RGC in attempt to preserve this key feature in visual information processing. Potential protein-targeting-motifs for the artificial recreation of the center-surround organization in the RGC dendritic field were examined.

METHODS

Viral construct:

Adeno-associated virus serotype 2 (AAV2/2) cassette with CAG (a hybrid CMV early enhancer/chicken B-actin) promoter and the channelrhodopsin-2 and GFP (ChR2-GFP) fusion construct (Bi et al., 2006) was modified by inserting the motif sequences at the 3’ end of GFP. These DNA constructs were packaged and affinity purified at the Gene Transfer Vector Core of the University of Iowa. DIO (double-floxed inverted open reading frame) constructs (Gradinaru et al., 2010) with the Ef1α (elongation factor-1 alpha) promotor was modified by inserting motif sequences at the 3’ end of ChR2-YFP or NpHR-YFP. DIO DNA constructs were packaged and affinity purified at the University of Pennsylvania.

Animal injection:

All animal experiments and procedures were approved by the Institutional Animal Care Committee at Wayne State University, and were in accord with the NIH Guide for the Care and Use of Laboratory Animals. Adult C57BL/6J mice or PCP2-*cre* transgenic mice aged 1–2 months were used for virus injections. Animals were anesthetized by intraperitoneal injection of ketamine (120 mg/kg) and xylazine (15 mg/kg). Under a dissection microscope, 1.0 µl of viral vector suspension was injected into the intravitreal space of each eye using a Hamilton syringe with a 32-gauge blunt-ended needle. Mice received viral vector injections at 1-4x10^{12} GP/ml. Animals were used for experiments at least one month after viral injection.

Fluorescence profile and morphological dendritic field measurements:

Animals were sacrificed by CO_2 asphyxiation followed by decapitation and enucleation for experiments. Enucleated eyes were fixed in 4% paraformaldehyde in phosphate buffer (PB) at room temperature (RT) for 20 minutes. XFP expression was examined in flat-mounted retinas. All images were acquired using a Zeiss Axioplan 2 microscope with Apotome (Carl Zeiss) with the AxioVision software. Z-stack images were taken at ~560 ms exposure time at optical

sections of 1 μm apart to capture the axon, soma, and the entire depth of the dendritic tree of each RGC. Images were exported for fluorescence intensity comparisons. Fluorescence intensity (FI) profiles were measured using the software ImageJ (obtained from NIH) by applying 5-pixel wide lines perpendicular to the cell membrane and averaging the peak FI measurements at the membrane. ImageJ fluorescence scale ranges from 0-225 where 0 corresponds to no fluorescence (black) and 225 corresponds to complete saturation (white). For each RGC, soma FI profile was obtained by averaging 3 measurements, dendrite FI profiles were obtained by averaging 9 measurements (3 proximal, 3 intermediate, and 3 distal dendrite measurements), and axon FI profile was obtained by averaging 3 measurements beyond the AIS. RGC morphological dendritic field sizes were assessed by approximating the GFP-positive dendritic tree area using the AxioVision software by outlining the outermost points of observed GFP fluorescence, rendering the outlined area into a circle then determining the diameter of that circle. Initial measurements were made in pixels which were converted into μm measurements.

Multielectrode array recordings:

Multielectrode array recordings were based on procedures reported by Tian and Copenhagen (2003). Briefly, the dissected retina was mounted photoreceptor side down on a piece of nitrocellulose filter paper (Millipore Corp., Bedford, MA). The mounted retina was placed in the MEA-60 multielectrode array recording chamber with the RGC layer touching the 10 μm diameter electrodes spaced 200 μm apart (Multi Channel System MCS GmbH, Reutlingen, Germany). During experiments, the retina was continuously perfused in 34°C oxygenated extracellular solution containing (in mM): NaCl, 124; KCl, 2.5; CaCl2, 2; MgCl2, 2; NaH2PO4, 1.25; NaHCO3, 26; and glucose, 22 (pH 7.35 with 95% O2 and 5% CO2). Recordings began approximately 60 min after placing the retina in the multielectrode array recording chamber. Signals were filtered between 200 Hz (low cut off) and 20 kHz (high cut off) and recorded by MC Rack software (Multi Channel Systems).

Light Stimulation:

For multielectrode array recordings, light stimuli were generated by a modified and laser-based LCD projector (8500, Espson). A 200 mW blue laser (473 nm) and a 300 mW green laser (532 nm) (Changchun New Industries Optoelectronics Tech.Co., Ltd., China)

were coupled via optical fiber to a projector which projected the stimuli to the bottom of the recording chamber. The projector rendered the 800 x 600 pixel (px) computer generated stimulus field into a 8 x 6 mm light stimulus field (6 x 10^{15} photons/cm^2 sec), therefore a 1 px corresponded to ~10 μm. Custom light pattern stimulation programs were designed in the Neurophysiology (Vision Research Graphics, Inc., Durham, NH, USA) software. The full-field program consisted of a 800 x 600 px stimulus. The stepping bar program consisted of a 200 x 6000 μm bar stimulus stepping at 20 μm increments. All light stimulation patterns were presented for 1 s followed by a 9 s inter-trial interval.

Physiological response field measurements:

Multielectrode array responses from individual neurons were analyzed using the Offline Sorter software (Plexon, Inc., Dallas, TX). The total number of steps that elicited ChR2-mediated spiking activity was determined then RGC response field size was multiplied by 20 μm/ 1 px to convert the response field into μm measurements for comparisons between groups.

Statistical analysis:

The Mann-Whitney test with post-hoc bonferroni correction was used for the pairwise comparisons. All statistical analyses were done using SPSS software.

RESULTS

In vivo motif-targeted ChR2-GFP expression in RGCs

In order for a cell to function effectively, its proteins must be accurately localized into proper subcellular compartments. For example, the precise distribution of voltage-gated sodium channels at the axon initial segment is crucial for action potential generation in the neuron (Kole et al., 2008). Localized proteins possess targeting-motifs within their amino acid sequences that serve as addresses of their proper final location. Motifs are recognized by intracellular trafficking machinery which transport and maintain the proteins at their specialized sites of function. This feature of subcellular targeting was utilized to investigate suitable motifs for the *in vivo* recreation of center and surround receptive fields within the RGC dendritic field. Motifs tested include six surround-targeting motifs: AMPAR-motif (Ruberti and Dotti, 2000), Kv4.2-motif (Rivera et al., 2003), MLPH-motif (Geething and Spudich, 2003; Lewis et al., 2009), nAChR-motif (Xu et al., 2006), NLG1-motif (Rosales et al., 2005), and TLCN-motif (Mitsui et al., 2005); and two center-targeting motifs: Kv2.1-motif (Lim et al., 2000) and Nav1.6-motif (Garrido et al., 2003; Boiko et al., 2003). All motifs are summarized in Table 1.

Center-targeting motifs

Kv2.1-motif: from voltage-gated potassium channel 2.1

3′-QSQPILNTKEMAPQSKPPEELEMSSMPSPVAPLPARTEGVIDMRSMSSIDS
FISCATDFPEATRF -5′

Nav1.6-motif: from voltage-gated sodium channel 1.6

3′-TVRVPIAVGESDFENLNTEDVSSESDP -5′

Surround-targeting motifs

AMPAR-motif: from AMPA receptor

3′-EFCYKSRSESKRMKGFCLIPQQSINEAIRTSTLPRNSGA -5′

Kv4.2-motif: from voltage-gated potassium channel 4.2

3′-FEQQHHHLLHCLEKTT -5′

nAchR-motif: from nicotinic acetylcholine receptor α7 subunit

3′-GEDKVRPACQHKPRRCSLASVELSAGAGPPTSNGNLLYIGFRGLEGM -5′

MLPH-motif: from melanophilin

3′-RDQPLNSKKKKRLLSFRDVDFEEDSD -5′

NLG1-motif: from neuroligin-1

3′-VVLRTACPPDYTLAMRRSPDDVPLMTPNTITM -5′

TLCN-motif: from telencephalin

3′-QSTACKKGEYNVQEAESSGEAVCLNGAGGGAGGAAGAEGGPEAAGGAAESP
AEGEVFAIQLTSA -5′

Table 1: Targeting motifs. Motif notation, origin protein, and motif amino acid sequences used in this study are summarized.

In vivo expression in the wildtype mouse (C57BL/6J) retina was achieved by intravitreal injection of adeno-associated virus serotype-2 (AAV2/2) carrying the ChR2-GFP gene. In constructs containing a targeting motif, the targeting sequence was inserted at the 3‘ end of GFP (Figure 7a and 7b: Constructs). In retinas injected with the non-targeted control construct, ChR2-GFP expression was observed on the membrane surface of the RGC somas, dendrites, and axons (Figure 7c). In retinas injected with center-targeting motifs, expression was markedly different from control. In the Kv2.1-motif injected retinas, expression was targeted mainly on the membrane surface of RGC soma, axon initial segment, and in some instances to proximal dendrites (Figure 7d). In the Nav1.6-motif injected retinas, expression was targeted mainly on the membrane surface of RGC soma, axon initial segment, and displayed a graded decrease in dendritic expression from proximal to distal dendrites (Figure 7e). In retinas injected with the surround-targeting motifs, expression was observed in RGC somas, dendrites, and axons to varying degrees (Figure 7f-k). In the MLPH-motif targeted RGCs, intracellular inclusions were consistently observed in the soma (Figure 7g: arrowheads).

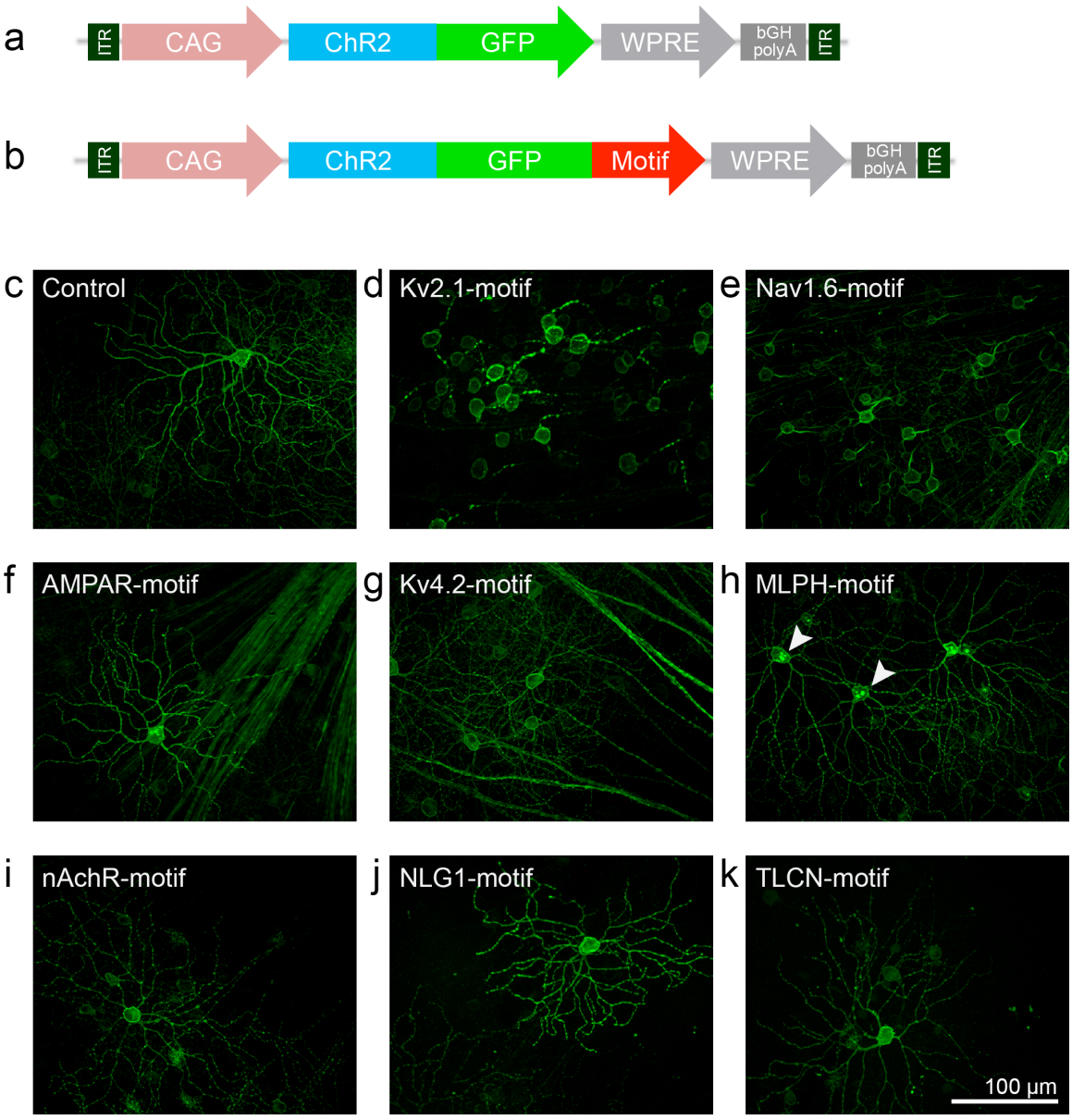

Figure 7: Viral constructs and expression in RGCs. **(a)** The control AAV2/2 viral construct carrying the ChR2-GFP gene and **(b)** the modified construct with targeting-motif inserted in the 3' end of GFP are driven by the ubiquitous CAG promoter. **c-k;** RGC expression of the ChR2-GFP **(c)** without motif targeting (control), with **(d)** Kv2.1-motif targeting, **(e)** Nav1.6-motif targeting, **(f)** AMPAR-motif targeting, **(g)** Kv4.2-motif targeting, **(h)** nAchR-motif targeting, **(i)** MLPH-motif targeting where soma inclusions are indicated by arrowheads, **(j)** NLG1-motif targeting, and **(k)** TLCN-motif targeting.

Degree of motif-mediated center- or surround-targeting

Suitability of each tested motif for center- or surround-targeting was determined by measuring the degree of polarization to the center or expression in the surround receptive filed of transduced retinal ganglion cells. Comparisons were made against cells that were transduced with the non-motif targeted control vector. At the same time, motifs that decreased axonal expression compared to control were preferred since the axon is not a natural part of the RGC receptive field.

Because all fluorescence images were obtained at similar exposure time, fluorescence intensity (FI) profiles taken from the soma, dendrites, and axon beyond the axon initial segment (AIS) were directly compared between the motif-targeted groups and the control group. Soma FIs for each motif-targeted group are as follows (mean ± SEM, median): Control: 146 ± 8, 150; Kv2.1: 118 ± 6, 117; Nav1.6: 75 ± 8, 73; AMPAR: 143 ± 9, 133; Kv4.2: 142 ± 9, 147; MLPH: 129 ± 9, 123; nAchR: 120 ± 5, 114; NLG1: 133 ± 7, 136; TLCN: 157 ± 16, 138. Soma FI profiles for all motif-targeted groups were similar to the control except the Nav1.6-motif group which had significantly lower FI ($p < 0.001$; Figure 8a). Dendrtite FIs for each motif-targeted group are as follows (mean ± SEM, median): Control: 65 ± 4, 68; Kv2.1: 2 ± 1, 0; Nav1.6: 11 ± 3, 5; AMPAR: 82 ± 4, 81; Kv4.2: 77 ± 5, 77;

MLPH: 74 ± 5, 78; nAchR: 67 ± 3, 69; NLG1: 76 ± 3, 76; TLCN: 53 ± 6, 39. Dendrite FI profiles for both center-targeted groups were significantly different than the control (Kv2.1-motif: $p < 0.001$; Nav1.6-motif: $p < 0.001$; Figure 8b) while there was no difference in the surround-targeted groups. Axon FIs for each motif-targeted group are as follows (mean ± SEM, median): Control: 37 ± 2, 38; Kv2.1: 19 ± 1, 16; Nav1.6: 25 ± 2, 26; AMPAR: 48 ± 3, 48; Kv4.2: 41 ± 3, 39; MLPH: 21 ± 2, 19; nAchR: 32 ± 2, 29; NLG1: 23 ± 2, 24; TLCN: 31 ± 3, 28. Axon FI profiles for both center-targeted groups were again significantly different than the control (Kv2.1-motif: $p < 0.001$; Nav1.6-motif: $p < 0.001$) along with two surround targeting motifs (MLPH-motif: $p < 0.001$; NLG1-motif: $p < 0.001$; Figure 8c).

For center-targeting, although both the Kv2.1-motif and the Nav1.6-motif had significantly lower dendrite and axon expression compared to control, the Nav1.6-motif had significantly lower soma expression. Therefore, the Kv2.1-motif was selected for center-targeting. For surround-targeting, while both the MLPH-motif and the NLG1-motif had significantly lower expression in the axon compared to control, the NLG1-motif was selected for surround targeting because the MLPH-motif resulted in intracellular inclusions. Note that although surround-targeted motif expression was observed in the entire dendritic tree and soma, the term “surround-targeting” will continue to

be used in this document in reference to NLG1-motif targeted expression. Despite expression in both dendrites and soma for surround-targeting which would overlap with the center-targeted zone, an antagonistic center-surround receptive field can still be generated as long as net excitatory and inhibitory zones exist.

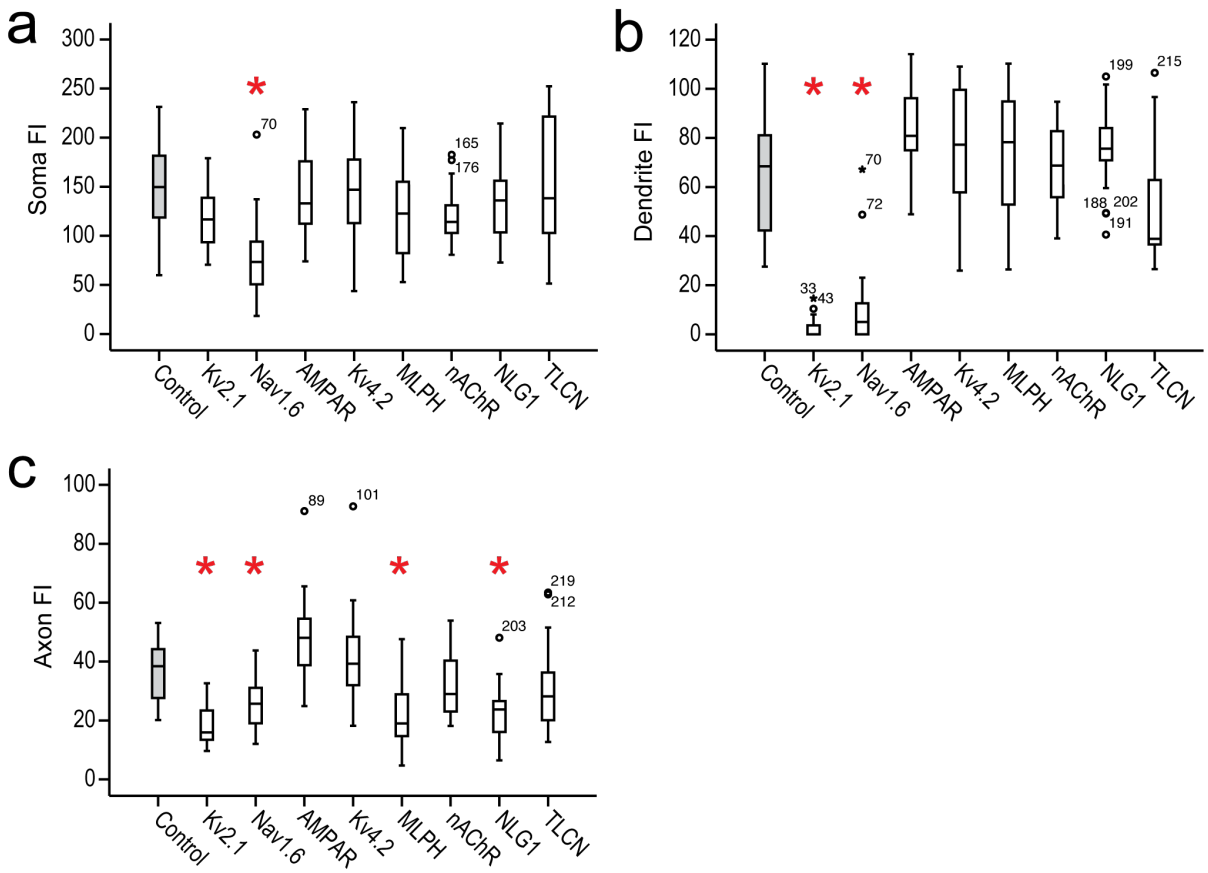

Figure 8: Fluorescence intensity (FI) comparisons between control and motif-targeted RGCs. GFP-FI profiles obtained from soma, dendrites, and axon of motif-targeted RGCs were compared to the non-targeted control expression (* $p < 0.001$). **(a)** Soma FI of Nav1.6-motif targeted expression was significantly different from control. **(b)** Dendrite FI of Kv2.1- and Nav1.6-motif targeted expression was significantly different from control. **(c)** Axon FI of Kv2.1-, Nav1.6-, MLPH-, and NLG1-motif targeted expression was significantly different from control.

Number of RGCs analyzed in each group are given in parentheses: Control (29), Kv2.1 (24), Nav1.6 (24), AMPAR (23), Kv4.2 (26), MLPH (25), nAchR (29), NLG1 (25), TLCN (19).

Morphological dendritic field size in PCP2-RGCs

To quantify the RGC morphological dendritic field size after center-targeting with the Kv2.1-motif and surround-targeting with the NLG1-motif, ChR2-YFP and NpHR-YFP expression were measured in a single population of RGCs. Limiting the study to a single type or RGC will limit the amount of variance in the results since the multiple types of RGCs have different dendritic field sizes and physiological properties. Therefore to achieve expression in one population of RGCs, the transgenic PCP2-*cre* mouse, which drives *cre*-inducible vector expression in only a single population of RGCs (Ivanova et al., unpublished data), was injected intravitreally with *cre*-inducible AAV2/2-DIO vectors (Figure 9a and b).

In the injected PCP2-*cre* retinas, ChR2-YFP and NpHR-YFP expression were observed in a single type of bistratified RGC (PCP2-RGC) and no other cell type (Elena et al., unpublished data). The ChR2-YFP, ChR2-YFP-NLG1-motif, and NpHR-YFP expression extended the entire dendritic tree in the PCP2-RGCs similar to that observed in wildtype retinas (Figure 9c, e, and f). However, the Kv2.1-motif resulted in strong targeting of the proximal dendrites in addition to the soma in the PCP2-RGCs (Figure 9d and g).

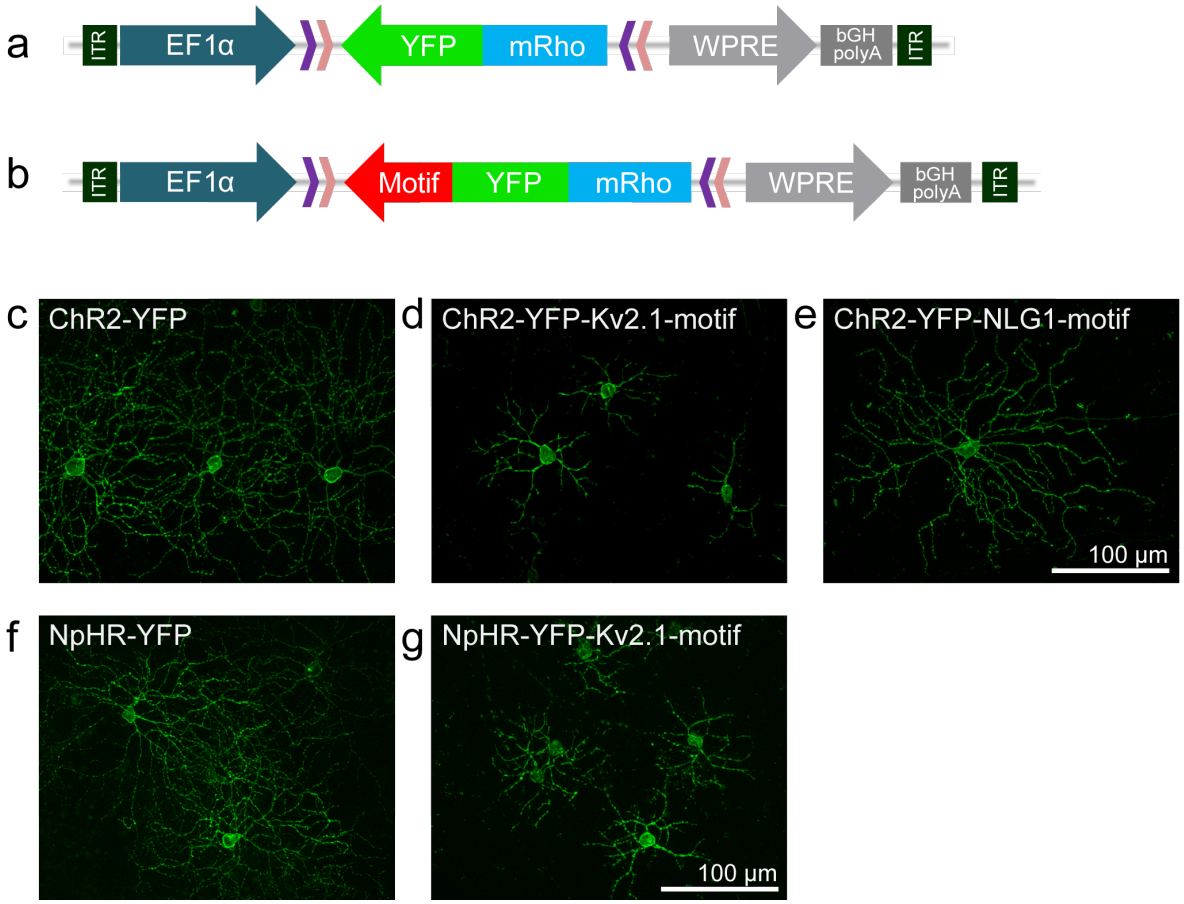

Figure 9: *Cre*-dependent viral constructs and expression in PCP2-*cre* RGCs. (a) The control AAV2/2-DIO construct carrying the microbial rhodopsin (mRho)-YFP gene and **(b)** the modified construct with targeting-motif inserted in the 3' end of YFP are driven by the ubiquitous Ef1α promoter. **c-e;** PCP2-RGC expression of the ChR2-YFP **(c)** without motif targeting (control), with **(d)** Kv2.1-motif targeting and with **(e)** NLG1-motif targeting. **f,g;** PCP2-RGC expression of the NpHR-YFP **(f)** without motif targeting (control) **(g)** and with Kv2.1-motif targeting.

In the non-targeted ChR2-YFP group, dendritic field expression diameter in PCP2-RGCs for the Kv2.1-motif (n = 33; mean ~75 ± 5 μm; median ~74 μm) and NLG1-motif (n = 27; mean ~242 ± 8 μm; median ~242 μm) were compared to the control (n = 30; mean ~239 ± 9 μm; median ~234 μm). The Kv2.1-motif resulted in a significantly different targeted dendritic field size ($p < 0.001$) while the NLG1-motif did not significantly differ compared to control (Figure 10a). In the NpHR-YFP group, targeted dendritic field diameter in PCP2-RGCs for the Kv2.1-motif (n = 23; mean ~82 ± 5 μm; median ~80 μm) were compared to the control (n = 23; mean ~221 ± 10 μm; median ~204 μm). The Kv2.1-motif resulted in a significantly different targeted dendritic field size ($p < 0.001$). NpHR-YFP-NLG1 data is not shown because the virus did not produce measurable expression.

By co-labeling with NpHR-YFP-Kv2.1 and ChR2-mCherry, we can provide proof of principle as to how the center-surround receptive field would be defined within a single RGC by this method (Figure 10b).

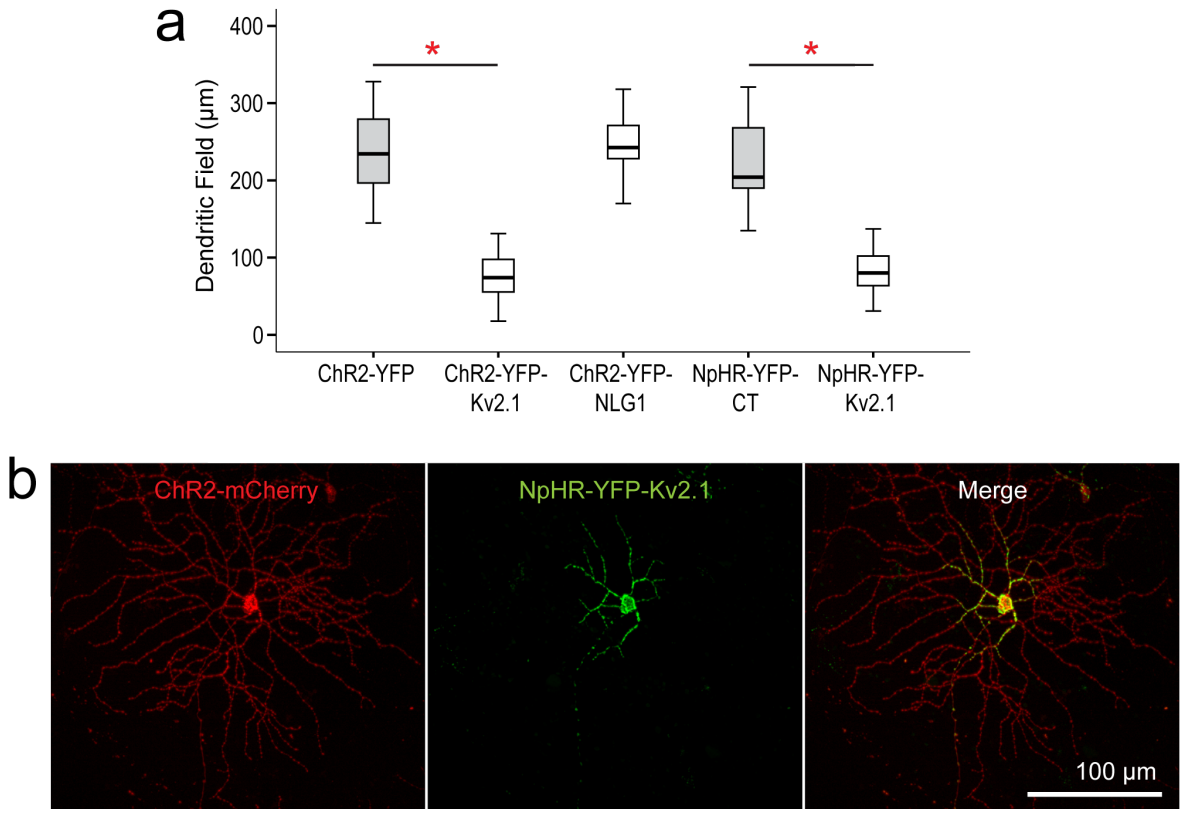

Figure 10: Motif-targeted dendritic field size. (a) Boxplot showing that in PCP2-RGCs, targeted dendritic field size of ChR2-YFP-Kv2.1-motif (ChR2-Kv2.1) was significantly different compared to ChR2-YFP (ChR2-CT). Targeted dendritic field size of NpHR-YFP-Kv2.1-motif (NpHR-Kv2.1) was significantly different compared to NpHR-YFP (NpHR-CT). * $p < 0.001$. **(b)** Co-expression of ChR2-mCherry and NpHR-YFP-Kv2.1 demonstrate a center-surround type organization in the dendritic field of a single RGC.

Physiological response field size in PCP2-RGCs

Since the Kv2.1-targeted-dendritic center receptive field is significantly smaller than the surround, how this targeting affected the physiological response field size in PCP2-RGCs was examined. Physiological response field size was assessed by multielectrode array recordings in retinal whole-mounts. All recordings were made under the condition that intrinsic photoreceptor light responses were blocked with L-AP4 and CNQX (6-cyano-7-nitroquinoxaline-2,3-dione) in order to isolate ChR2-mediated activity.

In all ChR2-YFP expressing retinas, ChR2 activity was confirmed with whole-field stimulation with a 1000 ms pulse of blue-green light (6×10^{15} photons/cm^2 sec) which elicited short-latency sustained ChR2-mediated spiking. After identifying a ChR2 expressing RGC, response field size was estimated by stepping a bar of light approximately 200 μm wide at 20 μm increments through the RGC receptive field. As the bar of light was stepped closer to the center of the RGC receptive field, spiking activity initiated more rapidly after light onset along with increasing spike frequency. Conversely, as the bar of light was stepped away from the receptive field center, spike activity initiation was more delayed and spike frequency decreased (Figure 11a-c). Spiking activity delays observed when the bar of light was at the RGC periphery may be because less of the dendritic field

was activated, therefore it may have taken a longer period of light exposure before enough ChR2 units were recruited and enough depolarization was generated to elicit spiking.

In all NpHR-YFP expressing retinas, NpHR activity was confirmed with whole-field stimulation with a 1000 ms pulse of blue-green light (6×10^{15} photons/cm^2 sec) which elicited short-latency NpHR-mediated rebound excitation spiking activity at light-off. After identifying an NpHR-expressing RGC, response field size was estimated by stepping a bar of light approximately 200 μm wide at 20 μm increments through the RGC receptive field. As the bar of light was stepped closer to the center of the RGC receptive field, rebound OFF-spiking activity initiated more rapidly after light onset along with increasing spike frequency. Conversely, as the bar of light was stepped away from the receptive field center, rebound OFF-spiking activity initiation was more delayed and spike frequency decreased (Figure 11d and e).

For each RGC, physiological response field size was estimated from the number of steps that elicited light-driven spiking activity and compared between the motif-targeted groups and the control. The estimated mean physiological response field size for the ChR2-YFP control was 1040 ± 92 μm (n = 13; median 920 μm), for the ChR2-YFP-Kv2.1-motif was 420 ± 74 μm (n = 11; median 380 μm), and for

the ChR2-YFP-NLG1-motif was 1317 ± 148 μm (n = 12; median 1330 μm). When compared to the ChR2-YFP-control, the ChR2-YFP-Kv2.1-motif resulted in a significantly different physiological response field size ($p < 0.0001$) while the ChR2-YFP-NLG1-motif did not show a difference (Figure 11f).

The estimated mean physiological response field size for the NpHR-YFP control was 935 ± 70 μm (n = 11; median 980 μm) and for the NpHR-YFP-Kv2.1-motif was 400 ± 48 μm (n = 10; median 370 μm). When compared to the NpHR-YFP-control, the NpHR-YFP-Kv2.1-motif resulted in a significantly different physiological response field size ($p < 0.0001$; Figure 11f).

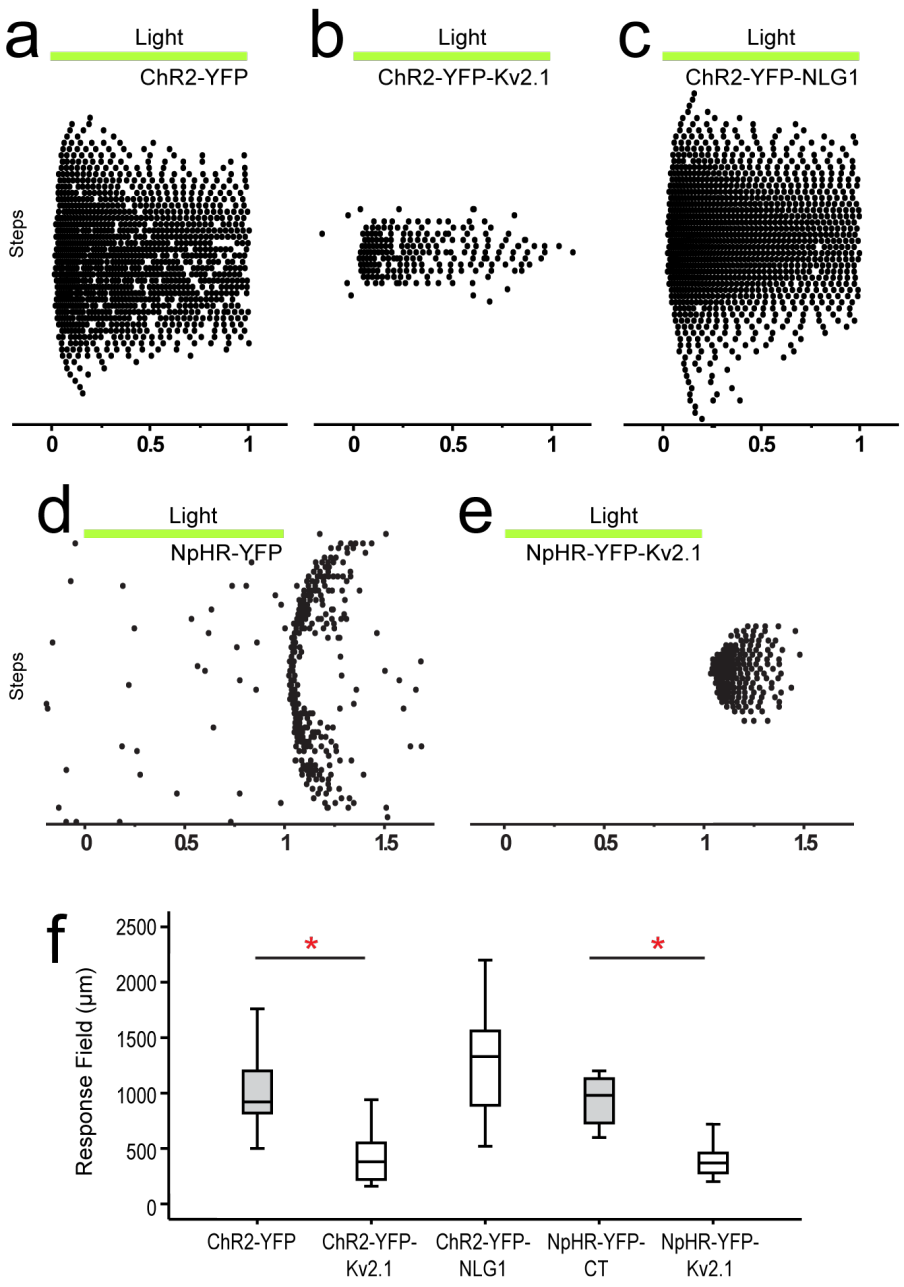

Figure 11: Motif-targeted response field size. a-c; Sample MCR traces of **(a)** ChR2-YFP, **(b)** ChR2-YFP-NLG1-motif, **(c)** ChR2-YFP-Kv2.1-motif, **(d)** NpHR-YFP **(e)** NpHR-YFP-Kv2.1-motif expressing PCP2-RGC to a 200 µm light bar stimulus stepping in 20 µm increments. Each row of dots represent spiking activity elicited by a 1s light pulse and sequential rows represent sequential steps through the RGC receptive field. **(f)** Boxplot showing both estimated ChR2- and NpHR-YFP-Kv2.1-motif targeted PCP2-RGC response field sizes are significantly different compared to non-targeted ChR2- and NpHR-YFP, respectively. * $p < 0.001$.

DISCUSSION

This study showed that *in vivo* motif-targeting can alter the subcellular localization of microbial rhodopsin-XFP in the RGC dendritic field as well as the physiological response field size. These results demonstrate that the Kv2.1-motif is feasible for generating a smaller center receptive field while the NLG1-motif is feasible for generating a larger encompassing surround receptive field within a single RGC while reducing axonal expression.

Morphological dendritic field and physiological response field discrepancy

This study found the estimated physiological response field measured by ChR2 light activation in the PCP2-RGC to be greater than their respective morphological dendritic field sizes. Even after accounting for the redundant response field activation due to the 200 μm bar stepping in 20 μm increments (-180 μm), response field sizes are still 6-7 times greater than dendritic field sizes of the respective groups. The enlarged physiological response field measurements could be due to scattering of the light beam as it passed through the multielectrode recording chamber and retinal tissue which could have widened the boundaries of the generated stimuli. Another reason could

be due to the reflection of the intense light stimulus off the white mounting filter paper which could also have resulted in a wider stimulus pattern. A wider bar stimulus would result in an increase in the physiological response field estimates for both center-targeting and surround-targeting constructs which is supported by the data. Another reason could be due to the light stimulation intensity used for the MCR recordings which was estimated to be ~10 times above threshold activation levels for the ChR2-GFP expressing RGCs. Above threshold light stimuli have been reported to result in enlarged estimation of receptive field size in the normal retina (Kuffler, 1953). The exact factors contributing to the dendritic field and response field size discrepancy are still under investigation; nonetheless, we still expect to be able to achieve a center-surround organization with the Kv2.1- and NLG1-motifs.

Differential expression of antagonistic opsins

The next step in creating an antagonistic center-surround receptive field directly in the RGC is to co-express ChR2 and NpHR. ON-center RGCs can be created by targeting ChR2 to the receptive field center with the Kv2.1-motif and by targeting NpHR to the surround with the NLG1-motif. Conversely, OFF-center RGCs can be

created by NpHR targeted to the center while ChR2 is targeted to the surround.

By expressing the antagonistic opsins ChR2 and NpHR into center and surround zones in the RGC dendritic tree, the center-surround antagonistic receptive field may be able to encode a new level of information that would otherwise not be possible through the expression of ChR2 or NpHR alone. Expressing only ChR2 or NpHR alone can render a cell into a luminance detector, however, as a recent study demonstrated in biolistically transfected RGCs of whole cultured rabbit retina, RGCs differentially expressing ChR2 in the dendrites targeted by PSD-95 and NpHR in the soma targeted by Ankyrin-G restored the ability for an RGC to encode edge information *ex vivo* (Greenberg et al., 2011). These findings could perhaps explain why expression of ChR2 alone in RGCs of the *Thy1* transgenic mice did not seem to improve vision in photoreceptor degenerated mice (Thyagarajan et al., 2010). Future *in vivo* studies of viral-mediated motif-targeted microbial rhodopsin therapy may offer insight into the effectiveness of center-surround reestablishment in vision restoration.

CHAPTER 4

FUTURE DIRECTIONS

Protein targeting motifs have been demonstrated to be a useful tool in studying action potential initiation in the AII amacrine cell and establishing a center-surround type receptive field organization directly in the RGC dendrites. Results from these studies have led to several unanswered questions which will require further investigation.

Further investigations of the AIS-like process of AII amacrine cells

AII-process synaptic connections and role in retinal function

AII-processes appear to be a unique and specialized extrusion of the AII amacrine cell. We now have evidence of it being the site of action potential generation, however, one intriguing question that is yet to be answered is whether these processes form synaptic connections with other neurons and, if so, what the identity of these neurons may be.

Additional evidence supporting the possibility of functional synaptic formation may have been provided in previous studies. In one study, synaptoporin staining in dissociated and isolated AII

amacrine cells not only showed expected heavy staining at the lobular appendages, but also at unexpected and consistent "hot spots," one per cell, outside the ascribed lobular appendage tree (Brandstatter et al., 1996). Recalling a peculiar finding where a never before seen chemical synapse was found in the ON-sublamina between a presynatpic AII amacrine cell process and a postsynaptic OFF-RGC dendrite (Strettoi et al., 1992), the authors posited that the "hot spots" could be sites of such rare synaptic formations (Brandstatter et al., 1996). Of the 21 lobular appendages examined in the OFF-sublamina, only two were found synapsed onto an RGC dendrite (Strettoi et al., 1992). From these reports, an attractive hypothesis could be that AII-processes form these minority synapses onto OFF-RGC dendrites. It is plausible that as the dendrites of OFF-RGCs course through the ON-sublamina in order to reach stratification in the OFF-sublamina, AII-processes are synapsing onto the dendrites throughout both levels of the IPL.

Future electron microscopy studies, especially with three-dimensional reconstruction of synaptic contacts (connectomes) may be especially helpful in elucidating these details. In a recent connectome reconstruction of retinal neurons, it was reported that AII amacrine cell lobular appendages formed synapses with OFF-RGCs, three populations of OFF-cone amacrine cells, and cone bipolar cells

(Anderson et al., 2011). Could one of these neurons be the synaptic partner of the AII-process as well? This information could help us more completely understand the complex roles of AII-amacrine cells in visual processing.

Future investigations of AII-process function

Future works could genetically manipulate AII amacrine cells on a population level by using transgenic mice. The transgenic *Fam81a* mouse line exhibits GFP expression in a large number of AII amacrine cells that covers the entire retina (Siegert et al., 2009). It would be interesting to investigate what effects ablation of AII amacrine cell spiking would have on the visual signaling of individual neurons, the retinal network, and perhaps even on the behavioral level. A potential experiment that may begin to address these question is to knock out Nav1.1 channel clustering in the AII amacrine cell. This can theoretically be achieved though reengineering the transgenic *Fam81a* mouse to express siRNA that interferes with Nav1.1 expression. If successful, the AII amacrine cell population in such a transgenic mouse model would be unable to produce action potentials. The consequences could then be studied to help us better understand the role of AII amacrine cells.

Implementation of artificial RGC center-surround antagonism

Practical considerations for microbial rhodopsin-based vision restoration therapy

The experiments were completed in mice but would most likely be reproducible in humans due to the commonalities of mammalian retinas. The adeno-associated virus (AAV) was selected as the delivery vehicle for gene delivery because of several advantageous properties. These include the lack of associated disease with the wild-type virus, the ability to transduce non-dividing cells such as retinal neurons, and the long-term expression of transgenes (Flotte, 2004; Sucrace and Auricchio, 2003). Hybrid AAV vectors containing an AAV-2 genome in an AAV-(1-9) capsid, named AAV-2/(1-9), have been produced for targeting different cells (Auricchio et al., 2001). In addition to viral serotype variations, cell type tropism can also be altered through cell specific promoters (Xu et al., 2001; Fitzsimons et al., 2002). AAV2/2 is the best characterized viral vector serotype currently used in clinical trials (Kay et al., 2000; Manno et al., 2003).

It is possible to create both ON-center and OFF-center RGCs by differential motif targeting. However, ways to selectively target only ON-center or only OFF-center RGCs are still under investigation. As knowledge about the unique gene profiles of ON-type and OFF-type

RGCs are elucidated, the ability to restrict gene expression in a single RGC subtype using distinct promotors becomes more promising.

Another factor to consider in the effort to improve microbial rhodopsin-based retinal prosthesis is light sensitivity. The ChR2 used in this study was ~5 log units less sensitive and NpHR was ~6 log units less sensitive than mammalian photoreceptors. This means significantly brighter light would be needed to activate these microbial rhodopsins. Furthermore, there are also limitations to the dynamic range of microbial rhodopsins. ChR2 responds to changes in illumination of ~2 log units. This range is limited in comparison with the mammalian retina that can respond to changes in illumination of ~10 log units as light levels vary from day to night. At the same time, because the sensitivity threshold is well above ambient light, these opsins will likely necessitate concomitant use of image processing hardware/software that can provide the light amplification and adjustment to represent the visual scene under different conditions.

Light sensitivity issues may also be addressed through discovery of new opsins, or by altering the kinetics of known microbial rhodopsins through genetic engineering. Current investigations into microbial opsins by mutagenesis have yielded several enhanced variants of both ChR2 (Kleinlogel et al., 2011, Lin et al., 2009; Berndt et al., 2009; Gunaydin et al., 2010), and HaloR (Zhao et al., 2008,

Gradinaru et al., 2008; Gradinaru et al., 2010) with improved speed and light sensitivity. The continual emergence of improved opsins combined with improving targeting techniques may advance the future of vision restoration efforts.

Beyond the retina

One advantage of targeting motifs is that their applications are not limited to the study of retinal neurons. It is conceivable that targeting motifs can be linked to a wide variety of fluorescent proteins to visualize neuron morphology with a new level of localization detail. Targeting motifs could also be linked with other neuromodulating proteins to manipulate neuron physiology.

REFERENCES

Abraham NM, Egger V, Shimshek DR, Renden R, Fukunaga I, Sprengel R, Seeburg PH, Klugmann M, Margrie TW, Schaefer AT, Kuner T (2010) Synaptic inhibition in the olfactory bulb accelerates odor discrimination in mice. Neuron 65:399-411.

Anderson JR, Jones BW, Watt CB, Shaw MV, Yang J-H, Demill D, Lauritzen JS, Lin Y, Rapp KD, Mastronarde D, Koshevoy P, Grimm B, Tasdizen T, Whitaker R, Marc RE (2011) Exploring the retinal connectome. Molecular vision 17:355-79.

Auricchio, A., Kobinger, G., Anand, V., Hildinger, M., O'Connor, E., Maguire, A., et al. (2001). Exchange of surface proteins impacts on viral vector cellular specificity and transduction characteristics: the retina as a model. Hum Mol Genet , 10:3075-3081.

Bamann C, Kirsch T, Nagel G, Bamberg E (2008) Spectral characteristics of the photocycle of channelrhodopsin-2 and its implication for channel function. Journal of Molecular Biology 375:686-694.

Baylor D (1996) How photons start vision. Proceedings of the National Academy of Sciences of the United States of America 93:560-565.

Berndt A, Yizhar O, Gunaydin LA, Hegemann P, Deisseroth K (2009) Bi-stable neural state switches. Nature Neuroscience 12:229-234.

Bi A, Cui J, Ma Y-P, Olshevskaya E, Pu M, Dizhoor AM, Pan Z-H (2006) Ectopic expression of a microbial-type rhodopsin restores visual responses in mice with photoreceptor degeneration. Neuron 50:23-33.

Blobel G, Walter P, Chang CN, Goldman BM, Erickson AH, Lingappa VR (1979) Translocation of proteins across membranes: the signal hypothesis and beyond. Symposia of the Society for Experimental Biology 33:9-36.

Blobel G (1980) Intracellular protein topogenesis. Proceedings of the National Academy of Sciences of the United States of America 77:1496-1500.

Bloomfield SA, Dacheux RF (2001) Rod vision: pathways and processing in the mammalian retina. Progress in Retinal and Eye Research 20:351-384.

Bloomfield S a, Xin D (2000) Surround inhibition of mammalian AII amacrine cells is generated in the proximal retina. The Journal of physiology 523:771-83.

Boiko T, Van Wart A, Caldwell JH, Levinson SR, Trimmer JS, Matthews G (2003) Functional specialization of the axon initial segment by isoform-specific sodium channel targeting. The Journal of neuroscience : the official journal of the Society for Neuroscience 23:2306-13.

Boos R, Schneider H, Wassle H (1993) Voltage-and transmitter-gated currents of all-amacrine cells in a slice preparation of the rat retina. Journal of Neuroscience 13:2874.

Boyden ES, Zhang F, Bamberg E, Nagel G, Deisseroth K (2005) Millisecond-timescale, genetically targeted optical control of neural activity. Nature Neuroscience 8:1263-1268.

Brandstätter JH, Löhrke S, Morgans CW, Wässle H (1996) Distributions of two homologous synaptic vesicle proteins, synaptoporin and synaptophysin, in the mammalian retina. The Journal of comparative neurology 370:1-10.

Caldwell JH, Daw NW (1978) Effects of picrotoxin and strychnine on rabbit retinal ganglion cells: changes in centre surround receptive fields. The Journal of Physiology 276:299-310.

Caldwell JH, Daw NW, Wyatt HJ (1978) Effects of picrotoxin and strychnine on rabbit retinal ganglion cells: lateral interactions for cells with more complex receptive fields. The Journal of Physiology 276:277-298.

Chang B, Hawes NL, Hurd RE, Davisson MT, Nusinowitz S, Heckenlively JR (2002) Retinal degeneration mutants in the mouse. Vision Research 42:517-525.

Cleland BG, Levick WR (1974) Properties of rarely encountered types of ganglion cells in the cat's retina and on overall classification. The Journal of Physiology 240:457-492.

Coombs JS, Curtis DR, Eccles JC (1957) The generation of impulses in motoneurones. The Journal of Physiology 139:232-249.

Crooks J, Kolb H (1992) Localization of GABA, glycine, glutamate and tyrosine hydroxylase in the human retina. Journal of Comparative Neurology 315:287-302.

Devries SH, Baylor DA (1997) Mosaic arrangement of ganglion cell receptive fields in rabbit retina. Journal of Neurophysiology 78:2048-2060.

Enroth-Cugell C, Robson JG (1966) The contrast sensitivity of retinal ganglion cells of the cat. The Journal of Physiology 187:517-552.

Famiglietti EVJ, Kolb H (1975) A bistratified amacrine cell and synaptic cirucitry in the inner plexiform layer of the retina. Brain Research 84:293-300.

Famiglietti EV, Kolb H (1976) Structural basis for ON-and OFF-center responses in retinal ganglion cells. Science 194:193-195.

Fitzsimons, H., Bland, R., & During, M. (2002). Promotors and regulatory elements that improve adeno-associated virus transgene expression in the brain. Method , 28:227-236.

Flotte, T. (2004). Gene therapy progress and prospects: recombinant adeno-associated virus (rAAV) vectors. Gene Ther , 11:805-10.

Garrido JJ, Giraud P, Carlier E, Fernandes F, Moussif A, Fache M-P, Debanne D, Dargent B (2003) A targeting motif involved in sodium channel clustering at the axonal initial segment. Science 300:2091-4.

Geething NC, Spudich JA (2007) Identification of a minimal myosin Va binding site within an intrinsically unstructured domain of melanophilin. The Journal of Biological Chemistry 282:21518-21528.

Gradinaru V, Thompson KR, Deisseroth K (2008) eNpHR: a Natronomonas halorhodopsin enhanced for optogenetic applications. Brain Cell Biol 36:129-139.

Gradinaru V, Zhang F, Ramakrishnan C, Mattis J, Prakash R, Diester I, Goshen I, Thompson KR, Deisseroth K (2010) Molecular and cellular approaches for diversifying and extending optogenetics. Cell 141:154-165.

Greenberg KP, Pham A, Werblin FS (2011) Differential targeting of optical neuromodulators to ganglion cell soma and dendrites allows dynamic control of center-surround antagonism. Neuron 69:713-20.

Grubb MS, Burrone J (2010) Activity-dependent relocation of the axon initial segment fine-tunes neuronal excitability. Nature 465:1070-1074.

Grunert U, Wassle H (1996) Glycine receptors in the rod pathway of the macaque monkey retina. Vis Neurosci 13:101-115.

Gunaydin LA, Yizhar O, Berndt A, Sohal VS, Deisseroth K, Hegemann P (2010) Ultrafast optogenetic control. Nature Neuroscience 13:387-392.

Han X, Boyden ES (2007) Multiple-Color Optical Activation, Silencing, and Desynchronization of Neural Activity, with Single-Spike Temporal Resolution. A. Rustichini, ed. PLoS ONE 2:12.

Hartline HK (1938) The response of single optic nerve fibers of the vertebrate eye to illumination of the retina. American Journal of Physiology 121:400-415.

Hartline HK (1940) The nerve messages in the fibers of the visual pathway. Journal of the Optical Society of America 30:239.

Hedstrom KL, Xu X, Ogawa Y, Frischknecht R, Seidenbecher CI, Shrager P, Rasband MN (2007) Neurofascin assembles a specialized extracellular matrix at the axon initial segment. The Journal of Cell Biology 178:875-886.

Ishizuka T, Kakuda M, Araki R, Yawo H (2006) Kinetic evaluation of photosensitivity in genetically engineered neurons expressing green algae light-gated channels. Neuroscience Research 54:85-94.

Ivanova E, Pan Z-H (2009) Evaluation of the adeno-associated virus mediated long-term expression of channelrhodopsin-2 in the mouse retina. Molecular Vision 15:1680-1689.

Kaneko Y, Watanabe S-I (2007) Expression of Nav1.1 in rat retinal AII amacrine cells. Neuroscience letters 424:83-8.

Kaplan E, Shapley RM (1986) The primate retina contains two types of ganglion cells, with high and low contrast sensitivity. Proceedings of the National Academy of Sciences of the United States of America 83:2755-2757.

Kay, M., Manno, C., Ragni, M., Larson, P., Couto, L., McClelland, A., et al. (2000). Evidence for gene transfer and expression of factor IX in haemophilia B patients treated wtih an AAV vector. Nat Genet , 24:275-61.

Kim CI, Leo MA, Lieber CS (1992) Retinol forms retinoic acid via retinal. Archives of Biochemistry and Biophysics 294:388-393.

Kleinlogel S, Feldbauer K, Dempski RE, Fotis H, Wood PG, Bamann C, Bamberg E (2011) Ultra light-sensitive and fast neuronal activation with the Ca2+-permeable channelrhodopsin CatCh. Nature Neuroscience 14:513-518.

Kole MHP, Ilschner SU, Kampa BM, Williams SR, Ruben PC, Stuart GJ (2008) Action potential generation requires a high sodium channel density in the axon initial segment. Nature neuroscience 11:178-86 .

Kuba H, Ishii TM, Ohmori H (2006) Axonal site of spike initiation enhances auditory coincidence detection. Nature 444:1069-1072.

Kuba H, Oichi Y, Ohmori H (2010) Presynaptic activity regulates Na+ channel distribution at the axon initial segment. Nature 465:1075-1078.

Kuffler SW (1953) Discharge patterns and functional organization of mammalian retina. Journal of Neurophysiology 16:37-68.

Lagali PS, Balya D, Awatramani GB, Münch TA, Kim DS, Busskamp V, Cepko CL, Roska B (2008) Light-activated channels targeted to ON bipolar cells restore visual function in retinal degeneration. Nature Neuroscience 11:667-675.

Lanyi JK (1986) Halorhodopsin: a light-driven chloride ion pump. Annual Review of Biophysics and Biophysical Chemistry 15:11-28.

Lanyi J, Luecke H (2001) Bacteriorhodopsin. Current Opinion in Structural Biology 11:415-419.

Lemaillet G, Walker B, Lambert S (2003) Identification of a conserved ankyrin-binding motif in the family of sodium channel alpha subunits. The Journal of Biological Chemistry 278:27333-9.

Levick WR (1967) Receptive fields and trigger features of ganglion cells in the visual streak of the rabbits retina. The Journal of Physiology 188:285-307.

Lewis TL, Mao T, Svoboda K, Arnold DB (2009) Myosin-dependent targeting of transmembrane proteins to neuronal dendrites. Nature Neuroscience 12:568-576.

Li X, Gutierrez DV, Hanson MG, Han J, Mark MD, Chiel H, Hegemann P, Landmesser LT, Herlitze S (2005) Fast noninvasive activation and inhibition of neural and network activity by vertebrate rhodopsin and green algae channelrhodopsin. Proceedings of the National Academy of Sciences of the United States of America 102:17816-17821.

Lim ST, Antonucci DE, Scannevin RH, Trimmer JS (2000) A novel targeting signal for proximal clustering of the Kv2.1 K+ channel in hippocampal neurons. Neuron 25:385-397.

Lin JY, Lin MZ, Steinbach P, Tsien RY (2009) Characterization of Engineered Channelrhodopsin Variants with Improved Properties and Kinetics. Biophysical Journal 96:1803-1814.

Lingappa VR, Lingappa JR, Blobel G (1980) Signal sequences for early events in protein secretion and membrane assembly. Annals Of The New York Academy Of Sciences 343:356-361.

Losonczy A, Makara JK, Magee JC (2008) Compartmentalized dendritic plasticity and input feature storage in neurons. Nature 452:436-441.

Mangel SC (1991) Analysis of the horizontal cell contribution to the receptive field surround of ganglion cells in the rabbit retina. The Journal of Physiology 442:211-234.

Manno, C., Chew, A., Hutchison, S., Larson, P., Herzog, R., Arruda, V., et al. (2003). AAV-mediated factor IX gene transfer to skeletal muscle in patients with severe hemophilia B. Blood , 101:2963-72.

Masland RH (2001) The fundamental plan of the retina. Nature Neuroscience 4:877-886.

Mazzoni F, Novelli E, Strettoi E (2008) Retinal ganglion cells survive and maintain normal dendritic morphology in a mouse model of inherited photoreceptor degeneration. Journal of Neuroscience 28:14282-14292.

Milam AH, Li ZY, Fariss RN (1998) Histopathology of the human retina in retinitis pigmentosa. Progress in Retinal and Eye Research 17:175-205.

Mitsui S, Saito M, Hayashi K, Mori K, Yoshihara Y (2005) A novel phenylalanine-based targeting signal directs telencephalin to neuronal dendrites. Journal of Neuroscience 25:1122-1131.

Münch T a, Silveira RA da, Siegert S, Viney TJ, Awatramani GB, Roska B (2009) Approach sensitivity in the retina processed by a multifunctional neural circuit. Nature neuroscience 12:1308-16.

Nagel G, Szellas T, Huhn W, Kateriya S, Adeishvili N, Berthold P, Ollig D, Hegemann P, Bamberg E (2003) Channelrhodopsin-2, a directly light-gated cation-selective membrane channel. Proceedings of the National Academy of Sciences of the United States of America 100:13940-13945.

Naka KI (1971) Receptive field mechanism in the vertebrate retina. Science 171:691-693.

Nelson R, Kolb H, Freed MA (1993) OFF-alpha and OFF-beta ganglion cells in cat retina. I: Intracellular electrophysiology and HRP stains. Journal of Comparative Neurology 329:68-84.

Olshevskaya EV, Calvert PD, Woodruff ML, Peshenko IV, Savchenko AB, Makino CL, Ho Y-S, Fain GL, Dizhoor AM (2004) The Y99C mutation in guanylyl cyclase-activating protein 1 increases intracellular Ca2+ and causes photoreceptor degeneration in transgenic mice. Journal of Neuroscience 24:6078-6085.

Palmer LM, Stuart GJ (2006) Site of action potential initiation in layer 5 pyramidal neurons. Journal of Neuroscience 26:1854-1863.

Pourcho R, Goebel D (1985) A combined Golgi and autoradiographic study of (3H)glycine-accumulating amacrine cells in the cat retina. Journal of comparative neurology 233:473-80.

Rivera JF, Ahmad S, Quick MW, Liman ER, Arnold DB (2003) An evolutionarily conserved dileucine motif in Shal K+ channels mediates dendritic targeting. Nature Neuroscience 6:243-250.

Rosales CR, Osborne KD, Zuccarino GV, Scheiffele P, Silverman MA (2005) A cytoplasmic motif targets neuroligin-1 exclusively to dendrites of cultured hippocampal neurons. European Journal of Neuroscience 22:2381-2386.

Ruberti F, Dotti CG (2000) Involvement of the proximal C terminus of the AMPA receptor subunit GluR1 in dendritic sorting. Journal of Neuroscience 20:RC78.

Russell TL, Werblin FS (2010) Retinal synaptic pathways underlying the response of the rabbit local edge detector. Journal of Neurophysiology 103:2757-2769.

Santiago Ramón y Cajal, Structure of the Mammalian Retina, 1900.

Santos A, Humayun MS, De Juan E, Greenburg RJ, Marsh MJ, Klock IB, Milam AH (1997) Preservation of the inner retina in retinitis pigmentosa. A morphometric analysis. Archives of ophthalmology 115:511-515.

Sassoe-Pognetto M, Wassle H, Grunert U (1994) Glycinergic synapses in the rod pathway of the rat retina: cone bipolar cells express the alpha 1 subunit of the glycine receptor. Journal of Neuroscience 14:5131-5146.

Shapley RM, Tolhurst DJ (1973) Edge detectors in human vision. The Journal of Physiology 229:165-183.

Shapley RM, Victor JD (1979) Nonlinear spatial summation and the contrast gain control of cat retinal ganglion cells. The Journal of Physiology 290:141-161.

Shapley R, Victor J (1986) Hyperacuity in cat retinal ganglion cells. Science 231:999-1002.

Sherman DL, Tait S, Melrose S, Johnson R, Zonta B, Court FA, Macklin WB, Meek S, Smith AJH, Cottrell DF, Brophy PJ (2005) Neurofascins are required to establish axonal domains for saltatory conduction. Neuron 48:737-742.

Siegert S, Scherf BG, Del Punta K, Didkovsky N, Heintz N, Roska B (2009) Genetic address book for retinal cell types. Nature neuroscience 12:1197-204.

Sineshchekov OA, Jung K-H, Spudich JL (2002) Two rhodopsins mediate phototaxis to low- and high-intensity light in Chlamydomonas reinhardtii. Proceedings of the National Academy of Sciences of the United States of America 99:8689-8694.

Strettoi E, Raviola E, Dacheux RF (1992) Synaptic connections of the narrow-field, bistratified rod amacrine cell (AII) in the rabbit. The Journal of Comparative Neurology 325:152–168.

Stryer L (1986) Cyclic GMP cascade of vision. Annual Review of Neuroscience 9:87-119.

Sucrace, E., & Auricchio, A. (2003). Adeno-associated viral vectors for retinal gene transfer. Prog Retin Eye Res , 22:705-19.

Suzuki T, Yamasaki K, Fujita S, Oda K, Iseki M, Yoshida K, Watanabe M, Daiyasu H, Toh H, Asamizu E, Tabata S, Miura K, Fukuzawa H, Nakamura S, Takahashi T (2003) Archaeal-type rhodopsins in Chlamydomonas: model structure and intracellular localization. Biochemical and Biophysical Research Communications 301:711-717.

Tamalu F, Watanabe S-I (2007) Glutamatergic input is coded by spike frequency at the soma and proximal dendrite of AII amacrine cells in the mouse retina. The European journal of neuroscience 25:3243-52.

Taylor WR (1999) TTX attenuates surround inhibition in rabbit retinal ganglion cells. Visual Neuroscience 16:285-290.

Thompson DA, Gal A (2003) Vitamin A metabolism in the retinal pigment epithelium: genes, mutations, and diseases. Progress in Retinal and Eye Research 22:683-703.

Thyagarajan S, Wyk M van, Lehmann K, Löwel S, Feng G, Wassle H (2010) Visual function in mice with photoreceptor degeneration and transgenic expression of channelrhodopsin 2 in ganglion cells. The Journal of Neuroscience 30:8745-58.

Tian M, Jarsky T, Murphy GJ, Rieke F, Singer JH (2010) Voltage-gated Na channels in AII amacrine cells accelerate scotopic light responses mediated by the rod bipolar cell pathway. Journal of neuroscience 30:4650-9.

Tian N, Copenhagen DR (2003) Visual stimulation is required for refinement of ON and OFF pathways in postnatal retina. Neuron 39:85-96.

Tomita H, Sugano E, Isago H, Hiroi T, Wang Z, Ohta E, Tamai M (2010) Channelrhodopsin-2 gene transduced into retinal ganglion cells restores functional vision in genetically blind rats. Experimental eye research 90:429-36.

Van Wart A, Boiko T, Trimmer JS, Matthews G (2005) Novel clustering of sodium channel Na(v)1.1 with ankyrin-G and neurofascin at discrete sites in the inner plexiform layer of the retina. Molecular and cellular neurosciences 28:661-73.

Van Wyk M, Taylor WR, Vaney DI (2006) Local edge detectors: a substrate for fine spatial vision at low temporal frequencies in rabbit retina. Journal of Neuroscience 26:13250-13263.

Van Wyk M, Wässle H, Taylor WR (2009) Receptive field properties of ON- and OFF-ganglion cells in the mouse retina. Visual Neuroscience 26:297-308.

Veruki ML, Hartveit E (2002a) AII (Rod) amacrine cells form a network of electrically coupled interneurons in the mammalian retina. Neuron 33:935-46.

Veruki ML, Hartveit E (2002b) Electrical synapses mediate signal transmission in the rod pathway of the mammalian retina. Journal of Neuroscience 22:10558-10566.

Werblin FS (1972) Lateral interactions at inner plexiform layer of vertebrate retina: antagonistic responses to change. Science 175:1008-1010.

Wiesel TN (1959) Recording inhibition and excitation in the cat's retinal ganglion cells with intracellular electrodes. Nature 183:264-265.

Xu J, Zhu Y, Heinemann SF (2006) Identification of sequence motifs that target neuronal nicotinic receptors to dendrites and axons. Journal of Neuroscience 26:9780-9793.

Xu, R., Janson, C., Mastakov, M., Lawlor, P., Young, D., Mouravlev, A., et al. (2001). Quantitative comparison of expression with adeno-associated virus (AAV-2) brain-specific gene cassettes. Gene Ther , 8:1323-32.

Zhang F, Wang L-P, Brauner M, Liewald JF, Kay K, Watzke N, Wood PG, Bamberg E, Nagel G, Gottschalk A, Deisseroth K (2007) Multimodal fast optical interrogation of neural circuitry. Nature 446:633-639.

Zhang Y, Ivanova E, Bi A, Pan Z-H (2009) Ectopic expression of multiple microbial rhodopsins restores ON and OFF light responses in retinas with photoreceptor degeneration. The Journal of Neuroscience 29:9186-96.

Zhao S, Cunha C, Zhang F, Liu Q, Gloss B, Deisseroth K, Augustine GJ, Feng G (2008) Improved expression of halorhodopsin for light-induced silencing of neuronal activity. Brain cell biology 36:141-154.

ABSTRACT

EXPRESSION OF MICROBIAL RHODOPSINS IN RETINAL NEURONS WITH SUBCELLULAR TARGETING MOTIFS: FOR THE STUDY OF THE STRUCTURE/FUNCTION OF AII AMACRINE CELLS AND FOR VISION RESTORATION

by

CHAOWEN WU

August 2011

Advisor: Dr. Zhuo-Hua Pan

Major: Anatomy & Cell Biology

Degree: Doctor of Philosophy

Protein-targeting motifs serve as addresses for subcellular protein localization. This feature of targeting-motifs was used to study the retina. The first part of the dissertation reports in the axonless spiking AII amacrine cell of the mammalian retina a dendritic process sharing organizational and functional similarities with the axon initial segment, the typical site of action potential initiation. This process was revealed through viral-mediated expression of channelrhodopsin-2-GFP (ChR2-GFP) with the AIS-targeting motif of sodium channels (NavII-III) and was shown to be the site of spike initiation. The second part of the dissertation aimed to improve microbial rhodopsin-mediated gene therapy for vision restoration by using targeting-motifs to recreate

center-surround antagonism in retinal ganglion cells (RGCs). Results of the study showed that a smaller center and a larger encompassing surround receptive field can be generated directly in a single RGC both morphologically and physiologically through the use of protein targeting motifs. Motif-targeting may be a promising approach in restoring center-surround antagonism in the RGC despite bypassing intraretinal processing.

AUTOBIOGRAPHICAL STATEMENT

I was born in China where I was taught the importance of structure and education. When I came to the United States at nine years old, I learned the importance of creativity and critical thinking. The Chinese part of me always knew I would pursue a PhD and I had the fortune of trying out various interests during my undergraduate education at the University of Michigan. After some trial and error, I realized my real passion and curiosity laid in studying the science behind how our bodies function, why they fail us, and how they can be fixed. That curiosity brought me into the MD-PhD program at Wayne State University School of Medicine where I was intrigued by the works of Dr. Zhuo-Hua Pan who was exploring an ingenious way to restore light sensitivity back into the blind retina using light-activated ion channels. The four years of my PhD was filled with cycles of excitement, doubt, high hopes, dashed hopes... but after this repetitive mental whiplash, my mind has emerged more flexible, faster, and stronger than ever.